Chapter 16
Primates from Senèze

Eric Delson

Abstract Senèze has yielded two primate fossils, neither from the recent field work. A partial ulna can be identified as cf. *Macaca sylvanus*. A nearly complete female skull is the holotype of *Dolichopithecus arvernensis* Depéret, 1928, now included in *Paradolichopithecus*. Emended and differential diagnoses are provided for this genus and species for the first time, and the Senèze skull is described and briefly compared to those of other species of the genus. Dental and cranial measurements are provided, along with comparative data. The macaque and *Paradolichopithecus* are moderately to highly terrestrial, respectively, and they suggest a woodland to more open environment. Senèze may be the youngest known occurrence of *Paradolichopithecus arvernensis*. A comparison of previous analyses results in retention of a *Paradolichopithecus-Macaca* link and of *Paradolichopithecus* and *Procynocephalus* as distinct genera.

Résumé Deux restes de Cercopithécidés fossiles sont connus à Senèze, ni l'un ni l'autre ne proviennent des fouilles récentes. Un fragment de cubitus est attribué à cf. *Macaca sylvanus*. Un crâne femelle sub-complet est l'holotype de *Paradolichopithecus arvernensis* (Depéret 1928). Nous retraçons un bref historique de la recherche sur le genre *Paradolichopithecus*. Nous présentons des diagnoses amendées de *Paradolichopithecus* et de *P. arvernensis*, accompagnées de comparaisons avec d'autres genres papionins. Le crâne de Senèze est décrit en détail. En se basant sur du matériel provenant d'autres sites nous pouvons dire que les squelettes postcrâniens de *Macaca* et de *Paradolichopithecus* sont adaptés à un habitus en partie ou totalement terrestre; cela suggère un paysage boisé relativement ouvert autour du maar de Senèze. Dans l'état actuel des connaissances, Senèze est peut-être le gisement le plus tardif ayant livré le genre *Paradolichopithecus,* vers 2,2–2,1 Ma. Compte tenu de sa taille légèrement plus petite, les spécimens de Grăunceanu sont probablement un peu plus ancien. Le spécimen d'individu femelle subadulte écrasé de Dafnero paraît de taille similaire, et une réévaluation des données paléomagnétiques publiées, suggèrent un âge compris entre 2,58 et 2,2 Ma.

Deux questions sur la systématique de *Paradolichopithecus* sont particulièrement discutées: est-il un synonyme de *Procynocephalus*, et est-il plus proche de *Macaca* ou de *Papio* ? La plupart des caractéristiques communes aux deux genres fossiles eurasiens sont basées sur une grande taille et une adaptation locomotrice terrestre, bien qu'elles diffèrent par la forme du dos du museau; de ce fait les deux genres sont maintenus comme distincts. De même, les caractéristiques suggérant un lien entre *Paradolichopithecus* et *Papio* (ou d'autres Papionina) semblent principalement liées à leur grande taille. Les arguments de distinctions ou de relations fondés sur le rapport de la surface de P4/M1 et à la forme du labyrinthe osseux ne résistent pas à un examen minutieux. Des analyses inédites de la morphométrie géométrique 3D et de cladistique des caractères du crâne tendent à montrer une relation entre *Paradolichopithecus* et *Macaca*.

Keywords *Paradolichopithecus arvernensis* • *Macaca sylvanus* • Cercopithecinae • Papionini • Macacina

E. Delson (✉)
Department of Vertebrate Paleontology, American Museum of Natural History, New York, NY, USA
e-mail: eric.delson@lehman.cuny.edu

Department of Anthropology, Lehman College of the City University of New York, Bronx, NY, USA

PhD Program in Anthropology, The Graduate Center of the City University of New York, New York, NY, USA

New York Consortium in Evolutionary Primatology, New York, NY, USA

Institut Català de Paleontologia Miquel Crusafont, Universitat Autònoma de Barcelona, Cerdanyola del Vallès, Barcelona, Spain

E. Delson et al. (eds.), *Senèze: Life in Central France Around Two Million Years Ago*, Vertebrate Paleobiology and Paleoanthropology, https://doi.org/10.1007/978-3-031-64415-3_16

Introduction

Only two primate specimens have been recovered at Senèze: one is a fragment of ulna, the other is a nearly complete skull, the holotype of a widespread species. This chapter will review the two specimens and discuss their taxonomic position and implications for paleoenvironment and relative age.

Note: upper teeth are indicated by uppercase letters, lower teeth by lowercase letters.

Institutional abbreviations: AMNH-M, American Museum of Natural History, Department of Mammalogy: AP, Sciences de la Terre, Faculté des Sciences, Université d'Alger, Algiers, Algeria: CMAI, Catedra de Morfologie si Antropologie, Universitatea 'Al. I. Cuza', Iasi, Romania; ERIS, Emil Racoviță Speleological Institute, Romanian Academy, Bucharest, Romania; FSL, Laboratoire de Paléontologie, Université Claude Bernard (UCB)-Lyon 1 (previously Faculty of Sciences, Lyon); ICP, Institut Català de Paleontologia Miquel Crusafont, Barcelona, Spain; LGPUT, Laboratory of Geology and Paleontology, University of Thessaloniki, Greece; MAP, Museo dell'Accademia del Poggio, Montevarchi, Italy; MNHN-Z-AC, Muséum national d'Histoire naturelle, Zoologie, Labo. Anatomie Comparée, Paris, France; NHCV, Natural History Collection, Museum of Vrissa, Lesvos, Greece; (now housed in Athens Museum of Paleontology and Geology; NMB, Naturhistorisches Museum Basel, Switzerland; NMP, Narodni Muzeum, Prague, Czech Republic; PIN-M, Institute of Paleontology, Russian Academy of Sciences, Moscow, Russia).

Previous Work on *Paradolichopithecus*

Delson and Plopsor (1975) and Szalay and Delson (1979) summarized the taxonomic history of this genus, including its frequent confusion with the colobine *Dolichopithecus*, which Depéret (1889) had described from Perpignan. In brief (updated here), Depéret (1928) reported the discovery of a "giant" relative of *Dolichopithecus* from Senèze, which he named *D. arvernensis*. This paper was delivered at the 1926 meeting of the International Geological Congress; it was rarely cited previously and never indicated as the original description of this species. The following year, Depéret (1929) described in detail the nearly complete skull and mandible of an adult female from Senèze, still considering that it was a later stage in a lineage including his Ruscinian species *D. ruscinensis*; in fact, Depéret linked the two more by size-related characters than by distinctive morphology. Verheyen (1962) first recognized that the narrow interorbital space, especially by comparison to the long muzzle, suggested that "*D.*" *arvernensis* was likely not a colobine but a cercopithecine. Vogel (1966, 1968) noted other features which placed this species in the Cercopithecinae, close to *Macaca*. Jolly (1967) reviewed the evolution of "baboons" (which he defined as large-bodied terrestrial cercopithecids) and followed Vogel and Verheyen, suggesting that *Dolichopithecus arvernensis* was a cercopithecine similar in cranial morphology to some macaques or possibly to the Asian *Procynocephalus*. Simons (1970) went a step further, suggesting that "*D.*" *arvernensis* should be included in *Procynocephalus*, perhaps in the type species *Pro. wimani* Schlosser (1924).

Meanwhile a partial face of a large monkey was one of the first fossils to be recovered from the Romanian site of Valea Grăunceanului (hereafter Grăunceanu), and Necrasov et al. (1961) described this as a new form similar to Depéret's *D. arvernensis*. They argued that it was probably colobine, but with some cercopithecine dental features, as well as the unique character of possessing a double supraorbital notch. This supposed double notch is, in fact, a single supraorbital notch, typical of larger cercopithecines, next to the broken region where the medial orbit margin turns down along the nasal bones; the damage probably confused Necrasov and colleagues, who were not primate specialists. They named the new genus and species *Paradolichopithecus geticus*, with this specimen as holotype. Simons (1970) recognized the similarity of this new species to "*D.*" *arvernensis* and suggested placing it also in *Procynocephalus*.

In 1971, Delson described a fragmentary juvenile mandible from the Spanish site of Cova Bonica and compared its large papionin dentition to those of extant *Papio* as well as "*D.*" *arvernensis* and *Paradolichopithecus geticus*, but only identified it as a large cercopithecine (cf. *Papio*). Delson and colleagues (Delson 1975; Delson & Plopsor 1975; Szalay and Delson 1979; Delson et al. 2000, 2014; Delson and Frost 2004; Ting et al. 2004; Frost et al. 2005) reviewed these and other finds, terming them *Paradolichopithecus arvernensis*, and employing *Paradolichopithecus* sp. for slightly smaller-bodied and geologically older specimens (see list below). Additional fossils of *P. arvernensis* were found at the Vatera-F site on Lesvos island (Greece; van der Geer & Sondaar 2002) and most recently at Dafnero-3 (Greece; Kostopoulos et al. 2018) and probably Karnezeika, Greece (two teeth and a fragment of radius; Sianis et al. 2023).

Meanwhile, Trofimov (1977) described several crania and mandibles from Kuruksay, Tajikistan, as *Paradolichopithecus sushkini*. These were discussed in more detail by

Maschenko (1994, 2005), who argued that *Paradolichopithecus* was phylogenetically close to or congeneric with *Papio*, while previous authors (e.g., Szalay and Delson 1979, Delson et al. 2000, Frost et al. 2005) had linked it with *Macaca* on the basis of facial shape. Qiu et al. (2004) named *Paradolichopithecus gansuensis* on the basis of a partial maxilla and mandible from Longdan (Gansu, China), suggesting that the teeth of *Paradolichopithecus* differed from those of *Procynocephalus*. These six localities (Grăunceanu, Vatera-F, Dafnero-3, Karnezeika, Kuruksay and Longdan) all appear to be similar in age (middle Villafranchian, MNQ 17, ca. 2.6–2.2 Ma), somewhat older than Senèze (dated 2.2–2.1 Ma, see Delson et al. 2024).

Another series of mostly fragmentary finds come mainly from still older sites, of late early Ruscinian to early Villafranchian age (ca. 4.3–2.6 Ma). Delson (1974) noted in a list (see also Szalay and Delson 1979 and Delson et al. 2000) that "*Dolichopithecus*" *arvernensis* was known from Malusteni (Romania) and Vialette (France). The former specimen was discussed as *D. ruscinensis* by Simionescu (1930), the latter was mentioned as an intermediate member of the "*Dolichopithecus*" lineage by Schaub (1943), but neither has yet been described in detail. Aguirre and Soto (1974, 1978) reported a juvenile partial mandible from La Puebla de Valverde (Spain). Moyà Solà et al. (1990) mentioned similar material from Moreda-1 (Spain), and Vlačiky (2009; see also Šujan et al. 2023) noted its presence at Nová Vieska (Slovakia). The most recent report of new material concerns three teeth from Ridjake, Serbia (Radović et al. 2019; 2024). All of these and the mandible and new specimens from Cova Bonica are attributed here to *Paradolichopithecus* sp. The origin of this lineage is unclear, whether from a European macaque or as the sister taxon to *Macaca*.

Meanwhile, in a series of papers, Nishimura and colleagues (2007, 2009, 2010, 2014) examined the facial morphology of *Paradolichopithecus* specimens from Kuruksay, Senèze and Longdan and the maxilla of *Procynocephalus wimani* from Xinan (Henan, China). They focused on the presence and extent of the maxillary sinus, which had been recognized in all extant species of *Macaca*, alone among modern cercopithecids. Of these, only "*P.*" *sushkini* presented a clear maxillary sinus. Nishimura et al. (2014) suggested that the maxillary sinus might be lost in some large macacinans due to development of the maxillary fossa.

In a brief abstract, Plastiras et al. (2017) termed the Dafnero specimen *Procynocephalus* without comment. Kostopoulos et al. (2018) suggested that the Dafnero cranium could be identified as either *Paradolichopithecus* or *Procynocephalus* and proposed that *Paradolichopithecus* is likely a junior synonym of *Procynocephalus*, following Jolly (1967) and Simons (1970). They also implied that *Paradolichopithecus* was more likely related to *Papio* than to *Macaca* (following Maschenko 1994, 2005).

Le Maître et al. (2023) analyzed the bony labyrinth morphology of the Dafnero specimen and other cercopithecines. Their results were not definitive, but they concluded that *Paradolichopithecus* showed similarities to Cercopithecini and Papionina, although not many to macaques. They suggested that *Paradolichopithecus* might be a stem papioninan or perhaps a basal papionin closer to Papionina than to *Macaca*.

Here I provide revised diagnoses of *Paradolichopithecus* and *P. arvernensis*, describe the Senèze specimen in detail and briefly analyze the fragmentary macaque ulna from the site. I also consider some of the above arguments in more detail (see Discussion below). Delson et al. (in preparation) will describe and analyze the fossils from Grăunceanu and Lesvos and place *Paradolichopithecus* in a broader context.

Systematic Paleontology

Order Primates Linnaeus, 1758
Semiorder Euprimates Hoffstetter, 1977
Hyporder Anthropoidea Mivart, 1864
Infraorder Catarrhini E. Geoffroy St. Hilaire, 1812
Parvorder Eucatarrhini Delson, 1977
Superfamily Cercopithecoidea Gray, 1821
Family Cercopithecidae Gray, 1821
Subfamily Cercopithecinae Gray, 1821
Tribe Papionini Burnett, 1828
Subtribe Macacina Owen, 1843
Genus *Macaca* Lacépède, 1799
cf. *M. sylvanus*, Linnaeus, 1758

Material: left partial ulna, NMB Se 1534, discovered in 1914, first reported by Stehlin (1923) as *Macaca* sp. Fragmentary specimen, with most of the proximal end and distal half broken away, but preserving the radial and distal part of the humeral articular surfaces. Figure 16.1 shows it in lateral view compared to a slightly larger ulna from Fornace RDB/Villafranca d'Asti (earliest Villafranchian) and a male extant *Macaca sylvanus*. The Senèze ulna is smaller than both others but may be a female (or possibly subadult if the distal epiphysis was unfused). The shaft appears straight and not curved, as also seen in the other two specimens, but the two fossils appear relatively more robust distal to the coronoid process compared to the extant specimen. Se 1534 presents less excavation or muscle markings laterally than the Fornace specimen or partial ulnae from the Upper Valdarno and Ain Mefta, or medially (posterior to the trochlear notch) than in the latter two ulnae or one from Zlaty Kun (see Table 16.1). This gracility again suggests a more lightly

built, possibly female individual. The preserved length of the bone is 93 mm, about half the length of a complete male or 55% of a complete female element of *Macaca sylvanus* (Table 16.1). Only two standard measurements can be taken on the Senèze ulna. Table 16.1 presents those values in comparison to extant and fossil *Macaca sylvanus* and the much larger *Paradolichopithecus arvernensis*. Those are the only two cercopithecid species known in Europe around 2 Ma, implying that the Senèze ulna can be identified as cf. *Macaca sylvanus*.

Genus *Paradolichopithecus* Necrasov, Samson and Rădulesco (1961).

Synonymy: *Dolichopithecus* Depéret, 1889, in part: Depéret (1928), Simionescu (1930); *Papio* Erxleben, 1777, in part: Delson (1971) (cf.), Aguirre and Soto (1974) (cf.), Maschenko (1994, 2005); *Procynocephalus* Schlosser, 1924, in part: Jolly 1967 (tentative), Simons (1970) (tentative), Kostopoulos et al. (2018) (tentative).

Type species: *Paradolichopithecus geticus* Necrasov, Samson and Rădulesco, 1961 (now generally accepted as a junior synonym of *Dolichopithecus arvernensis* Depéret, 1928).

Other included species: *Paradolichopithecus* sp. Delson and Plopsor (1975) (Vialette, France; Moreda 1A, Cova Bonica, La Puebla de Valverde, Spain; Malusteni, Romania; Nová Vieska, Slovakia; Ridjake, Serbia); possibly also

Fig. 16.1 *Macaca sylvanus* left ulnae in lateral views, left to right: NMB VJ 130 partial proxinal ulna from Fornace RDB (right side photographically reversed); NMB Se 1534, fragmentary proximal ulna from Senèze; extant specimen from North Africa, Naturalis (Leiden)

"*Paradolichopithecus*" *sushkini* Trofimov, 1977 (Kuruksay, Tajikistan) and "*Paradolichopithecus*" *gansuensis* Qiu, Deng and Wang, 2004 (Longdan, Gansu, China); see discussion below.

Emended diagnosis (formalized and modified in part after Szalay and Delson 1979): Large papionin comparable in size to larger subtaxa of extant *Papio*. Distinguished by combination of smooth median dorsal profile without anteorbital drop, rounded and slightly peaked (not flattened) transverse muzzle dorsum and nasals, little to no facial fossae or maxillary ridges and known postcranial elements (especially forelimb and phalanges) indicative of highly terrestrial locomotion.

Differential diagnosis (see also Gilbert 2013): *Paradolichopithecus* is distinguished from *Dinopithecus, Gorgopithecus*, *Mandrillus*, *Papio*, *Pliopapio*, *Soromandrillus* and *Theropithecus* by the lack of a defined anteorbital drop in the midline facial profile; *Cercocebus, Lophocebus, Macaca, Parapapio, Procercocebus* and *Rungwecebus* also lack an anteorbital drop. Distinguished from *Dinopithecus, Gorgopithecus*, *Mandrillus*, *Papio* and *Soromandrillus* by rounded (and slightly "peaked") rather than flattened transverse muzzle dorsum; similar in this region to *Pliopapio* and to some *Cercocebus, Lophocebus, Macaca, Parapapio*, *Procercocebus*, *Rungwecebus* and *Theropithecus* (all variable); differs from *Procynocephalus*, which has a more flattened middle part of muzzle dorsum (breakage prevents observation of anteorbital region). Similar to *Macaca* and *Procynocephalus* (and variably *Dinopithecus, Parapapio* and *Pliopapio*) but distinguished from *Cercocebus, Gorgopithecus*, *Lophocebus, Mandrillus*, *Papio*, *Procercocebus*, *Rungwecebus*, *Soromandrillus* (possibly variable in later Omo and Angolan samples) and *Theropithecus* (other than most *T. oswaldi*) by the absence of a maxillary fossa and mandibular corpus fossa. Distinguished from *Macaca* (and "*P.*" *sushkini*) by lack of a maxillary sinus. Distinguished from *Mandrillus*, *Papio*, *Procercocebus*, *Soromandrillus*, most fossil *Theropithecus* and (morphology variable) *Cercocebus, Lophocebus* and *Parapapio* in lacking male maxillary ridges. Distinguished from *Cercocebus, Parapapio, Pliopapio*, *Procercocebus*, *Rungwecebus* and (variably) *Lophocebus* and *Macaca* by prominent and horizontally oriented supraorbital torus in males; in *Gorgopithecus* also prominent but anteroinferiorly oriented, downturned in midline. Distinguished from *Cercocebus, Mandrillus*, *Procercocebus* and *Soromandrillus* by anteriorly converging temporal lines, rather than more divergent, more posteriorly converging lines. Distinguished from *Gorgopithecus* by vertical rather than anteroposteriorly curved upper incisor roots. Distinguished from *Theropithecus* by simpler molar structure lacking elevated and complex enamel folding. The p4/P4 is not typically enlarged relative to the m1/M1 as it is in *Cercocebus, Mandrillus*, and some (geochronologically younger) *Soromandrillus*, but more as in *Lophocebus, Papio* and at least some *Macaca* (although there is some overlap of ranges in extant taxa, see Table 16.2 and Fig. 16.2). Distinguished from *Cercocebus, Lophocebus, Macaca, Parapapio, Pliopapio* and *Rungwecebus* but broadly similar to *Mandrillus*, *Papio*, *Procercocebus* (probably), *Procynocephalus* and *Theropithecus* by strongly terrestrial/cursorial adaptations of the forelimb such as robust humerus with medial epicondyle well retroflexed and medial trochlear

Table 16.1 Comparative ulnar measurements (in mm) of extant and fossil *Macaca sylvanus* and *Paradolichopithecus arvernensis*

Specimen, locality, reference	Age	Sex	Length	APThTN	WRA
Macaca sylvanus					
NMB Se 1534, Senèze	eEPl	f?	93 (b)	10.5	14.0
AP 1A7 Ain Mefta, Algeria (Pomel, 1896)	lMPl	?		13.0	15.0
NMP unnumbered, Zlaty Kun Cave 718, Czech Republic (Vlcek, 1961)	mMPl	f?		10.5	13.2
ICP 14956, Terrassa, Spain (Alba et al. 2008; specimen not yet published)	lEPl	m?		11.3	14.0
MAP 12, Upper Valdarno (Terranova Bracciolini), Italy (Gentili et al., 1998; not yet published)	mEPl	m?		11.7	14.4
NMB VJ 130, Fornace RDB (Villafranca d'Asti), Italy (Rook et al., 2001)	LP	m?		13.4	15.8
MNHN-Z-AC, 1910.166, extant	modern	m	185.1	14.5	15.8
MNHN-Z-AC 1900.244, extant	modern	f	167.4	11.4	14.1
MNHN-Z-AC 1899.52, extant	modern	m	186.0	14.2	17.2
AMNH-M 185,277, extant	modern	f	168.9	11.6	12.5
Paradolichopithecus arvernensis					
ERIS VGr/350 b, Grăunceanu, Romania (Szalay and Delson 1979)	eEPl	m?		20.0	21.0
NHCV PO 059 F, Vatera-F, Lesvos, Greece (van der Geer and Sondaar 2002)	eEPl	m?		20.3	–
NHCV PO 229 F, Vatera-F, Lesvos, Greece (van der Geer and Sondaar 2002)	eEPl	m?		20.6	23.4

Age abbreviations: l,. L–late; m, M–middle; e, E–early; Pl–Pleistocene; P–Pliocene. Sex: f, female; m, male. All measurements by ED on originals.
Length: (proximal surface of olecranon to distal tip of styloid process ("head"); b: measurement of broken length as preserved.
APThTN: anteroposterior thickness of the trochlear notch in the (proximo-distal) middle of the notch;
WRA: width across the radial articulation from the coronoid tip to the lateral margin

"crest" expanded distally; ulnar olecranon large and somewhat tilted posteriorly; partial femora robust; and phalanges stout (relevant postcrania unknown in *Dinopithecus, Gorgopithecus* and *Soromandrillus*). Distinguished from *Cercocebus, Lophocebus, Macaca, Parapapio, Pliopapio*, *Procercocebus*, *Rungwecebus* and smaller subtaxa of *Papio* and *Theropithecus* in size and broadly comparable to *Dinopithecus, Gorgopithecus*, *Mandrillus*, larger subtaxa of *Papio*, *Soromandrillus,* and mid-sized subtaxa of *Theropithecus* (as indicated by tooth and skull size and estimated mass: females ca. 15–23 kg, males ca. 18–40 kg, from Delson et al. 2000).

Description: The cranial midline profile descends from glabella in a smooth, hollow curve to rhinion, which projects slightly, and then more steeply and almost linearly to prosthion. The flanks of the maxilla and mandibular corpus are

Table 16.2 Comparative dental measurements (in mm) of *Paradolichopithecus*, *Papio* and *Mandrillus*

Taxon/specimen	I1 W	I1 L	I1 H	I2 W	I2 L	I2 H	C W f	C L f	C H f	P3 W f	P3 L f	P4 W	P4 L
P. arvernensis Senèze FSL 41333	7.1	7.7	6.9	6.6	5.5	9.8	7.9	8.2	13.2	9.0	7.0	9.9	7.3
P. arvernensis Grăunceanu CMAI unnumbered	8.5	8.2	10.7	7.8	8.2	11.6	6.5	9.0	14.1	7.9	7.4	9.0	8.3
P. arvernensis Dafnero-3 LGPUT DFN-3 150 (right side)										7.1	6.9	7.9	7.8
"*P." sushkini* Kuruksay PIN-M 3120–523				7.2	7.3	9.5	7.0	8.6	16.3	8.0	7.4	9.6	7.6
Papio h. ursinus Mean	9.28	9.63		7.91	7.2		6.65	8.54		7.23	6.99	8.72	7.85
Papio h. ursinus N	130	132		116	117		57	57		61	61	144	146
Papio h. ursinus Max	11.9	11.6		10.0	8.7		8.1	12.3		8.3	8.6	10.3	9.8
Papio h. ursinus Min	6.8	6.4		5.6	5.1		4.8	5.9		6.1	5.7	7.0	6.1
	M1AW	M1PW	M1 L	M2AW	M2PW	M2 L	M3AW	M3PW	M3 L	I1 A	P4 A	M1 A	P4/M1 A
P. arvernensis Senèze FSL 41333	10.2	9.6	10.8	12.8	11.0	13.3	12.8	10.7	13.7	54.7	72.27	110.16	0.66
P. arvernensis Grăunceanu CMAI	10.0	9.7	12.1	12.1	10.9	12.9	12.4		14.3	69.7	74.7	121.0	0.62
P. arvernensis Dafnero-3 LGPUT	9.4	8.9	10.8	10.6	11.4	13.4	11.7	10.2	13.5		61.6	101.5	0.61
"*P." sushkini* Kuruk PIN-M 3120–523	11.7	10.7	13.3	14.0	12.4	14.7	14.8	12.2	14.2		72.96	155.61	0.47
Papio h. ursinus Mean	10.0	9.34	11.13	11.87	10.95	13.48	12.34	10.69	13.91	89.1	68.82	111.47	0.62
Papio h. ursinus N	171	170	173	160	159	160	141	141	141		143	171	145
Papio h. ursinus Max	12.0	11.0	13.1	13.7	12.9	15.5	14.2	13.1	16.4		94.9	140.2	0.81
Papio h. ursinus Min	8.7	8.0	8.35	9.5	9.0	10.4	10.2	8.2	10.1		43.9	72.8	0.48
	i1 W	i1 L	i1 H	i2 W	i2 L	i2 H	c W f	c L f	c H f	p3 W f	p3 Lf	p4 W	p4 L
P. arvernensis Senèze FSL 41333	7.0	4.8	6.8	3.6	7.5	6.4	9.8	6.4	12.4	6.4	10.9	7.2	8.4
P. arvernensis Grăunceanu CMAI							8.2	4.9	11.7	5.3	10.1	8.7	9.3
P. arvernensis Vatera NHCV PO 170 F	6.67	5.39	10.2	6.09	5.53	9.5	7.7	5.57	14.13	5.37	9.9	7.11	8.67
Papio h. ursinus Mean	8.64	7.28		7.99	6.23		8.23	5.01		5.12	12.17	7.00	8.88
Papio h. ursinus N	118	120		120	119		59	59		61	61	133	137
Papio h. ursinus Max	10.3	8.6		9.8	8.0		9.7	5.8		6.2	16.1	8.4	10.6
Papio h. ursinus Min	6.5	4.3		5.9	3.6		7.1	4.3		4.4	9.0	5.7	7.0

(continued)

Table 16.2 (continued)

Taxon/specimen	m1AW	m1PW	m1 L	m2AW	m2PW	m2 L	m3AW	m3PW	m3 L	p4 A	m1 A	p4/m1 A
P. arvernensis Senèze FSL 41333	8.6	8.5	10.1	10,5	10.0	12.4	10,8	10.4	17.8	60.48	86.86	0.70
P. arvernensis Grăunceanu CMAI	8.6	8.7	11.3	11.0	10.9	13.3	10.6	10.1	16.5	80.91	97.18	0.83
P. arvernensis Vatera PO 170 F	8.2	8.09	9.87	10.5	9.44	13.25	11.08	9.48	17.84	61.64	80.93	0.76
Papio h. ursinus Mean	8.2	8.56	10.68	10.38	9.97	13.09	11.29	10.22	16.74	62.71	87.95	0.72
Papio h. ursinus N	157	158	164	146	148	150	134	133	133	132	157	127
Papio h. ursinus Max	9,6	9.9	12.4	12.5	11.9	15.3	13.2	11.6	19.4	84.8	112.2	0.95
Papio h. ursinus Min	6.4	6.8	8.0	8.7	7.9	10.1	9.2	8.1	13.2	43.4	55.2	0.51
	P4 A	M1A	P4/M1 A							p4 A	m1A	p4/m1 A
Mandrillus sp. Mean	71.97	92.4	0.78							62.24	74.31	0.85
Mandrillus sp. N	48	52	48							66	69	46
Mandrillus sp. Max	109.2	125.9	0.95							90.4	102.0	1.31
Mandrillus sp. Min	48.9	72.4	0.53							34.2	53.5	0.43

Fossil specimens all judged female. *P. arvernensis* Senèze and Grăunceanu, *P. sushkini* Kuruksay original measurements; Dafnero from Kostopoulos et al. (2018)

Papio hamadryas ursinus and *Mandrillus* sp. from PRIMO (http://primo.nycep.org; original measurements by Delson, Eisenhart and colleagues); all mixed-sex other than canine and P3/p3 values limited to female specimens (f).

Upper teeth indicated by uppercase letters (I, C, P, M), lower teeth by lowercase letters (I, c, p, m), L = maximum mesiodistal length: measured on c perpendicular to W; measured on p3 as projected maximum parallel to alveolar plane from distal margin to mesialmost end of flange. W = buccolingual width: measured on incisors at cervix; measured on C perpendicular to L; on c, this is maximum dimension at cervix due to rotation of canine in jaw. AW = buccolingual width across mesial loph(id); PW = buccolingual width across distal loph(id). A = area; premolar area is product of L x W; molar area is product of L x AW (following Fleagle and McGraw 1999, 2002). N, number of specimens measured; Max, maximum; Min, minimum.

smooth and generally unhollowed by fossae, but this is variable, especially on the mandible. The muzzle is grooved below the orbits for vessels exiting the infraorbital foramina. There is no maxillary sinus (except in "*P.*" *sushkini*, which might suggest inclusion in a distinct genus); the maxillary body is thin at the level of P3-M1 or M2, but may be thicker in males at M3; the zygomatico-maxillary suture occurs at the level of M3. Cranial sexual dimorphism may be low compared to extant African papionins of similar size, but lack of both male and female specimens from the same locality makes this difficult to demonstrate. The supraorbital torus is strongly built in both sexes, running nearly horizontally above the orbits before turning rather sharply inferiorly at the lateral margins; glabella is slightly protruding. The neurocranium is somewhat more globular in females and more elongate in males. The temporal lines run medially and posteriorly from the lateral end of the supraorbital torus. In females, they are nearly parallel and diverge slightly as they merge into the moderate nuchal crest. In males, they meet near the inferred position of bregma to form a low sagittal crest which again diverges slightly as it merges with the nuchal crest, which is relatively flat, not upturned in the midline. The endocast was described as typically cercopithecine in sulcal patterns, if with a slightly lower occipital region (Radinsky 1974).

The mandibular corpus is of moderate and constant depth; the ramus is somewhat posteriorly inclined. The dentition is typically papionin, with large front teeth and moderate molar flare. Lower molars show a variable degree of "crestiness" of lophids, even at similar stages of wear. The ratio of fourth premolar to first molar area is comparable to values in *Papio, Macaca* and *Lophocebus*, somewhat lower than the means for *Mandrillus* and *Cercocebus*. The humerus is robust with a well retroflexed medial epicondyle and distally expanded medial trochlear "crest"; the ulnar olecranon is large and somewhat tilted posteriorly; partial femora are robust; and phalanges are stout.

Paradolichopithecus arvernensis (Depéret, 1928)

Synonymy: *Dolichopithecus arvernensis* Depéret, 1928: *Paradolichopithecus geticus* Necrasov, Samson and Rădulesco, 1961; "*Dolichopithecus*" *arvernensis* Depéret, 1928: Simons (1970), Delson (1974); *Procynocephalus* sp. cf. *P. wimani* Schlosser, 1924: Simons (1970); *Paradolichopithecus arvernensis* (Depéret, 1928): Delson (1975).

Holotype: FSL 41336, nearly complete female skull.

Type locality: Senèze (Haute-Loire, France), ca. 2.2–2.1 Ma, late Villafranchian, MNQ 18 (see Delson et al. 2024, Crégut-Bonnoure et al. 2024).

Hypodigm: numerous specimens from Grăunceanu (Romania) and Vatera-F (Lesvos, Greece) and probably one or two specimens each from Dafnero-3 and Karnezeika (Greece); not listed here as not from Senèze.

Emended diagnosis: A large species of *Paradolichopithecus* broadly comparable in size to larger subtaxa of extant *Papio* (e.g., samples of *P. h. anubis* and *P. h. ursinus*). Estimated mass (Delson et al. 2000) is ca. 25–40 kg for males (combining dental, cranial and postcranial estimates) and around 15–23 kg for females (dental only). These values are similar to those for "*P.*" *sushkini* from Kuruksay but larger than for male *Paradolichopithecus* sp. from Cova Bonica (and probably other sites noted above) at ca. 18–25 kg. Selected dental measurements for female specimens of *P. arvernensis* and "*P.*" *sushkini* are provided in Table 16.2, along with comparative values for a large sample of *Papio hamadryas ursinus* and area ratios of P4/M1 and p4/m1 for these taxa and also *Mandrillus sphinx* which has relatively large fourth premolars (Fleagle and McGraw 1999, 2002; Gilbert 2007, 2013).

Figure 16.2 is a box plot of P4/M1 area ratios in large samples of three mixed-sex groups of mainly extant papionins: *Cercocebus* and *Mandrillus*; *Papio*, *Lophocebus* and *Theropithecus* (including some fossils of the latter); and *Macaca*; plus selected individuals of *Paradolichopithecus* and *Procynocephalus* (details in figure caption). The boxes for the *Cercocebus* and *Mandrillus* (C-M) and *Papio*, *Lophocebus* and *Theropithecus* (P-L–T) groups do not overlap; the former have larger values indicating their relatively larger P4s. Macaques mainly fall between those two groups, the boxes overlapping slightly. *Paradolichopithecus arvernensis* overlaps macaques and the P-L–T group. "*Paradolichopithecus*" *sushkini* has quite small P4s, overlapping only the P-L–T lower whisker. *Procynocephalus subhimalayanus* lines up with the macaques but also the lower C-M and upper P-L–T whiskers, while "*Paradolichopithecus*" *gansuensis* lies lower on the plot. The fossils mostly align with macaques (and P-L–T), indicating moderately-sized P4 compared to M1.

Figure 16.3 is a box plot of M3 area in a selection of mixed-sex extant and fossil larger papionins. *Paradolichopithecus* and *Procynocephalus* species overlap extant large *Papio*, are generally larger than *Mandrillus* and overlap the smaller individuals of the large African fossil species. *Macaca sylvanus* is clearly the smallest of these taxa, much smaller than the larger extant *Papio* subspecies and the

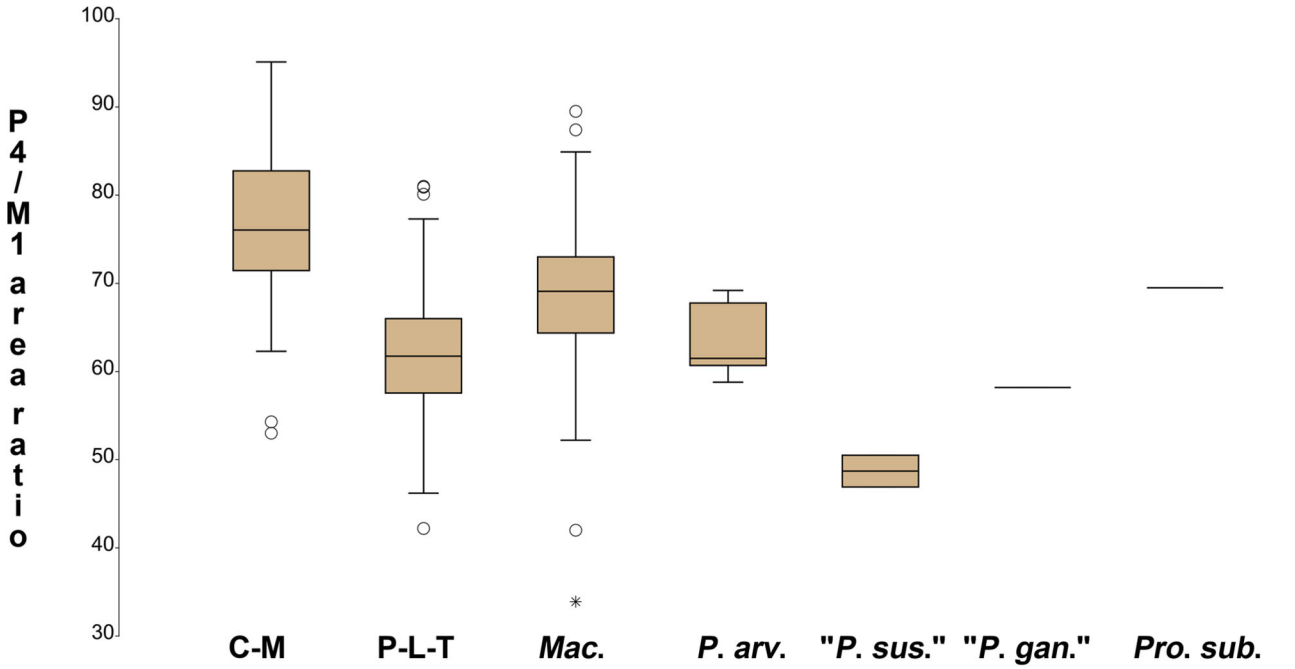

Fig. 16.2 Box plot of P4/M1 area ratio in percent (100 × P4 width x P4 length/M1 mesial width x M1 length) in selected mixed-sex mainly extant papionins: C-M, *Cercocebus* spp. (40 specimens) and *Mandrillus* spp. (48 specimens); P-L–T, *Papio* sspp. (211 specimens), *Lophocebus* spp. (51 specimens), *Theropithecus* spp. (32 T. *gelada*, 12 fossil *T. oswaldi* sspp.); *Mac.*, *Macaca* spp. (48 M. *sylvanus* specimens, 50 specimens of various other species). The focal fossils include: *P. arv.*, *Paradolichopithecus arvernensis* from Senèze (1 specimen), Grăunceanu (6 specimens) and Dafnero-3 (1 specimen); "*P.*" *sus.*, "*Paradolichopithecus*" *sushkini* (2 specimens); "*P.*" *gan.*, "*Paradolichopithecus*" *gansuensis* (1 specimen); *Pro. sub.*, *Procynocephalus subhimalayanus* (1 specimen). Boxes show 25% and 75% quartiles, horizontal line inside the box is the median; whiskers are drawn from the top (or bottom) of the box to the largest (smallest) data point less than 1.5 times the box height outside the box; outlier values beyond the whiskers are indicated as circles, while those more than 3 times the box height outside the box are indicated as asterisks. Data from PRIMO (http://primo.nycep.org) and Table 16.2

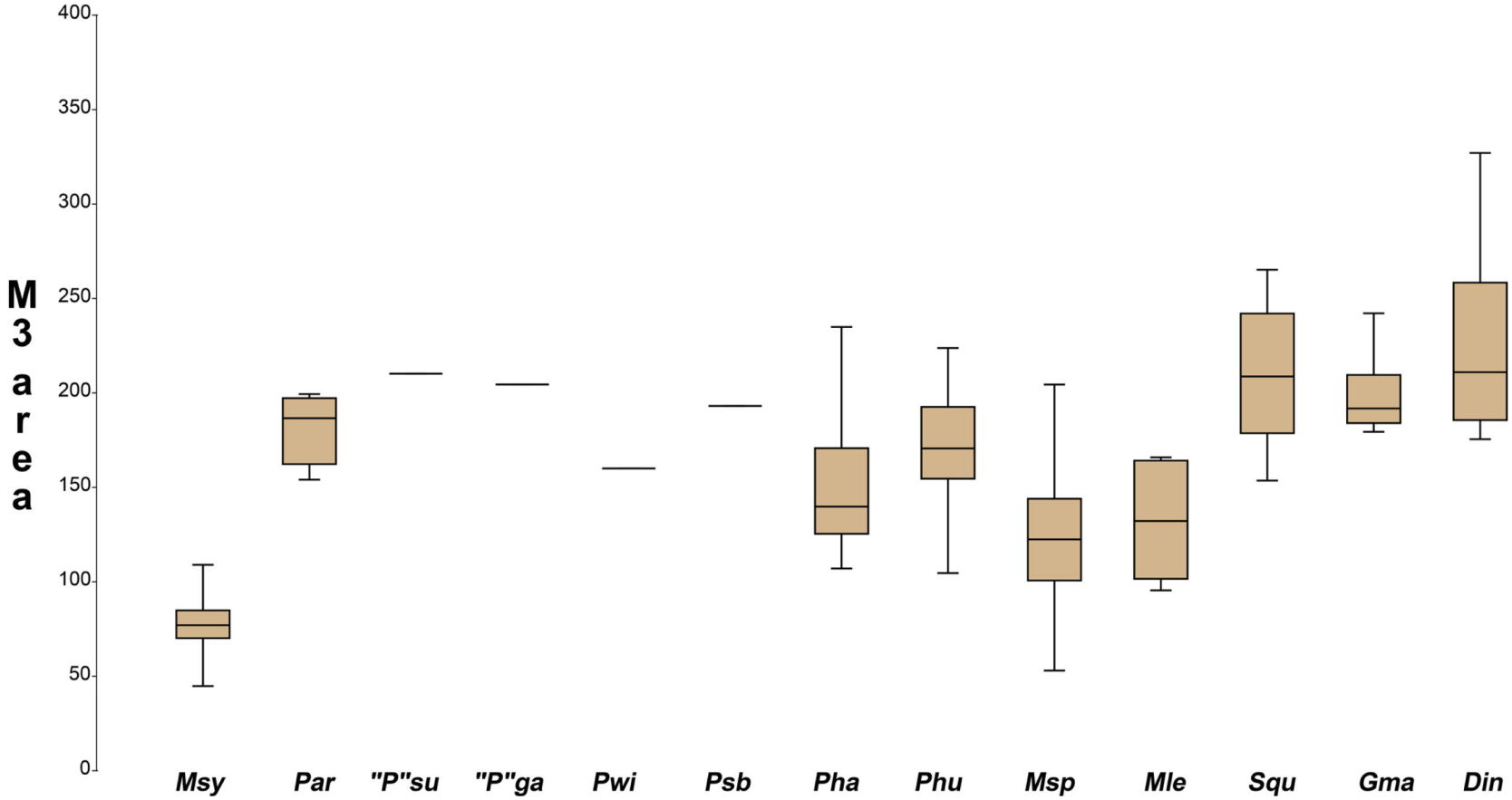

Fig. 16.3 Box plot of M3 area in cm^2 (M3 mesial width x M3 length) in selected mixed-sex mainly extant larger papionins (fossil taxa marked with †): *Msy*, *Macaca sylvanus* (50 specimens); *Par*, *Paradolichopithecus arvernensis* † from Senèze (1 specimen), Grăunceanu (6 specimens) and Dafnero-3 (1 specimen); "*P˜su*, "*Paradolichopithecus*" *sushkini* † (1 specimen); "*P'ga*, "*Paradolichopithecus*" *gansuensis* † (1 specimen); *Pwi*, *Procynocephalus wimani* † (1 specimen); *Psb*, *Procynocephalus subhimalayanus* † (1 specimen); *Pha*, *Papio hamadryas anubis* (30 specimens); *Phu*, *Papio hamadryas ursinus* (141 specimens); *Msp*, *Mandrillus sphinx* (26 specimens); *Mle*, *Mandrillus leucophaeus* (11 specimens); *Squ*, *Soromandrillus quadratirostris* † (12 specimens); *Gma*, *Gorgopithecus major* † (8 specimens); *Din*, *Dinopithecus ingens* † (7 specimens). Boxes show 25% and 75% quartiles, horizontal line inside the box is the median; whiskers are drawn from the top (or bottom) of the box to the largest (smallest) data point. Data from PRIMO (http://primo.nycep.org) and Table 16.2

fossils plotted, overlapping only the smallest *Mandrillus sphinx*; it is among the largest macaques and shows that a significant increase in size must have accompanied the origin of the Eurasian fossil taxa.

Table 16.3 provides selected measurements (defined in Table 16.4) on female skulls of the same taxa. The original Grăunceanu female face (Necrasov et al. 1961) does not permit many skull measurements to be taken, but two are essentially identical to the Senèze specimen: upper molar row length 40.6 mm and buccal jaw depth below m3 at 29 mm. The cranium from Senèze does not have a maxillary sinus (those from Grăunceanu are under study), nor does that of "*P.*" *gansuensis* from Longdan, as opposed to those of "*P.*" *sushkini* which have sinuses. The maxillary body is thin at the level of P3-M2 but moderately thick at M3 (in the Senèze holotype but thin in males from Grăunceanu), again similar to "*P.*" *gansuensis* but different from "*P.*" *sushkini* (which is thick at P3-M2 but thin at M3). Neither females nor males present more than minimal maxillary or mandibular corpus fossae, as opposed to moderately developed ones in "*P.*" *sushkini* and "*P.*" *gansuensis*.

Detailed Description of Senèze Skull

General. FSL 41336 was partly reconstructed from numerous fragments by Depéret (1929). This reconstruction was taken apart and re-restored after cleaning and more careful alignment by Battetta (1969), who made a cast of the restoration (Fig. 16.4) and then disarticulated the specimen into fourteen fragments, most of which do not cleanly contact one another. The canine roots (absolutely short but longer than the crown) combined with the small p3 confirm identification as a female.

The largest cranial fragment comprises the nearly complete braincase and part of the upper face (Figs. 16.5 and 16.6). Lacking from this region are: part of the right temporal (including the petrous region, the external auditory meatus and zygomatic process); the right occipital condyle; and the antero-lateral portion of the right frontal, behind which the bone is damaged along the right side of the coronal suture. Most of the left malar is present on this piece, completing the lateral half of the orbit rim. Another fragment includes almost all of the right malar and the adjacent anterolateral part of the frontal (a space remains near the external corner of the orbit, although a carved piece of plaster fills it in casts). The fronto-malar segment makes a loose contact with a fragment comprising the posterior portion of the temporal process of the malar firmly sutured to the anterior two-thirds of the malar process of the temporal (together making up about half of the right zygomatic arch). Two yet smaller elements almost complete the connection to the neurocranium at the root of the malar process. Another small fragment nearly closes the right orbit inferiorly, between the malar and the maxilla.

The second largest cranial fragment is composed of the majority of the right maxilla and teeth, part of the left maxilla and portions of the premaxillae and nasals (Fig. 16.7). The right maxilla extends almost to the malar and ethmoid margins along the inferior border of the orbit; there are two areas of damage inferiorly, above the M1-2 contact and on the inferior part of the premaxillary suture alongside the nasal aperture. The palatal roof is almost entirely missing on both sides. The inferior two-thirds of the nasal bones (probably damaged at rhinion) contact a small slip of the right premaxilla next to the nasal aperture. Another segment of the premaxilla contains the right I2 and abuts the maxillary toothrow with C-M3. The superior portion of the left maxilla is present as an elongate strip along the nasal bones and aperture to above the canine alveolus, but a large region is missing from above the molars past the zygo-maxillary suture up to the inferior orbit margin and frontal. The three left molars are conjoined in one fragment of alveolar margin, while the anterior segment of premaxilla with I1-2 and a portion of internal maxillary wall with P3-4 form another. The right I1 and left C are isolated.

The mandible is almost completely preserved, except for the left i2 and an area of external surface bone posterior and inferior to the right canine root (Figs. 16.8 and 16.9). It is broken into two portions between the right canine and p3. A piece of external corpus below the p3 and abutting (and covering) the canine root was never recovered, while some of the corpus base inferior to this was previously attached to the larger segment but is currently missing. The two parts of the corpus make poor contact and have not been glued together.

Dentition. The teeth are heavily worn but clearly papionin in morphology (Figs. 16.7, 16.8 and 16.9). The upper canine is short from apex to cervix, and the root of the isolated left C is taller than the crown. This is typical of papionin females. The P3 flange is slightly longer than that of the P4. The molar buccal notches are shallow. The lower canine crown is slender and looks like those of males, but the root (clearly visible on the left where the corpus is broken off, see Fig. 16.9) is still taller and curved distally. This shape is different from the smaller crowns of the *P.* "*geticus*" holotype and Vatera PO 170 F. The p3 flange (in all three mandibles) extends just slightly below the alveolar plane. The p4-m3 lingual notches are worn but shallow.

Face. The reconstructed face has a moderately steep but curving anteorbital drop and a tall maxilla above the alveolar plane (Figs. 16.4 and 16.10). The orbits have a straight superior margin below fairly thick brows, then curving smoothly down both medially and laterally to zygomax superior, where the zygomaticomaxillary suture crosses the

Table 16.3 Comparative skull measurements (in mm) of female *Paradolichopithecus arvernensis* and *Papio hamadryas anubis* (variables defined in Table 16.4)

Taxon/Specimen	NAIN	NABA	NABR	NAPR	NARH	BAIN	BABR	BAPR	PRIN	PRBR	PRRH	PROB	INOB	ZMOB
P. arvernensis Senèze FSL 41333	115.0	78.5	68.0	96.5	46.0	52.0	64.0	128.0	180.0	155.0	54.0	85.5	116.0	27.5
P. arvernensis Dafnero-3 LGPUT DFN3-150	120.1 d			84 d	45.5				171.3 d					
Papio h. anubis females Mean	99.49	73.32	57.07	79.97	45.40	48.73	62.00	111.53	154.48	133.83	35.83	70.93	94.19	30.75
Papio h. anubis females N	13	11	2	2	2	2	2	2	2	2	2	2	2	2
Papio h. anubis females Maximum	107.6	79.5	57.9	83.9	52.8	50.9	63.4	111.8	158.1	138.2	39.2	72.7	98.3	31.8
Papio h. anubis females Minimum	91.7	66.3	56.3	76.0	38.0	46.5	60.6	111.2	150.9	129.4	32.5	69.2	90.1	29.7
	BIPG	MAXW	FACH	BIZY	TMIN	PORB	BIOR	INOR	ORBH	ORBW	SUPO	FORW	FORL	NASW
P. arvernensis Senèze FSL 41333	76.7	81.8	82.5	118.0	12.0	48.2	101.0	14.0	27.8	32.5	8.1	15.0	15.0	22.0
P. arvernensis Dafnero-3 DFN3-150						39.8 d	63.4 d	9.0 d	26.5 d	26.7 d		12.8 d	18.5 d	
Papio h. anubis females Mean	74.56	73.87	62.52	97.33	28.73	54.09	68.11	4.51	23.43	28.99	3.77	16.69	17.76	19.10
Papio h. anubis females N	2	2	2	2	2	4	4	2	4	4	2	2	2	2
Papio h. anubis females Maximum	77.1	78.5	64.3	100.3	38.7	55.6	75.6	5.2	24.8	30.2	3.9	17.4	18.4	20.2
Papio h. anubis females Minimum	72.1	69.2	60.7	94.4	18.8	52.5	59.9	3.8	21.3	27.3	3.7	16.0	17.1	18.0
	NASL	BMEU	I1MU	I1AU	M3IU	M3PU	M3MU	ALWU	PDEP	AFAC	IDCO	SYML	PLAL	GNAL
P. arvernensis Senèze FSL 41333	35.5	61.5	15.5	14.0	75.0	50.8	38.6	15.8	10.5	40.0	128.5	40.5	29.5	22.5
P. arvernensis Dafnero-3 DFN3-150						50.9	37.7							
P. arvernensis Vatera NHCV PO 170 F												37.2	21.8	19.1
Papio h. anubis females Mean	26.84	50.29	16.18	17.46	70.98	47.61		13.52	7.16	36.00	112.09	35.61	22.49	19.84
Papio h. anubis females N	2	4	2	2	2	2		4	2	2	2	2	2	2
Papio h. anubis females Maximum	29.0	56.8	18.0	19.7	74.3	49.8		15.7	7.6	36.0	115.7	39.7	23.6	20.6
Papio h. anubis females Minimum	24.7	45.1	14.4	15.2	67.6	45.4		12.3	6.7	36.0	108.5	31.5	21.4	19.1
	BICO	RAML	CORH	BJD3	BJD4	ALWL	M3IL	I1AL	I1ML	ARAM	ASYM	ORBW/NAIN	FACH/BIOR	BIOR/NAIN
P. arvernensis Senèze FSL 41333	80.0	35.5	70.0	34.4	34.2	14.6	76.5	9.5	10.3	115.0	130.0	28.3	81.7	87.8
P. arvernensis Dafnero-3 DFN3-150														
P. arvernensis Vatera PO 170 F				28.1	29.9	13.1	70.4							
Papio h. anubis females Mean	72.09	33.37	57.14	21.81	26.06	12.02	71.45	11.19	12.53	105.50	131.50	30.6	83.3	72.0
Papio h. anubis females N	2	2	2	2	2	4	2	2	2	2	2	4	2	4
Papio h. anubis females Maximum	72.8	34.2	59.9	23.0	28.1	14.0	75.9	12.7	14.2	108.0	135.0	32.0	85.0	81.2
Papio h. anubis females Minimum	71.4	32.5	54.4	20.7	24.0	10.3	67.0	9.6	10.9	103.0	128.0	28.9	81.5	63.4

Data sources: *P. arvernensis* Senèze and Vatera original measurements; Dafnero from Kostopoulos et al. (2018; specimen crushed bilaterally, values with "d" are distorted from original values); all female individuals.

Papio hamadryas anubis from PRIMO (http://primo.nycep.org; original measurements by Delson and colleagues); limited to female specimens

Table 16.4 Definition of skull measurements in Table 16.3

NAIN	Nasion to Inion
NABA	Nasion to Basion
NABR	Nasion to Bregma
NAPR	Nasion to Prosthion (= Alveolare)
NARH	Nasion to Rhinion
BAIN	Basion to Inion
BABR	Basion to Bregma
BAPR	Basion to Prosthion
PRIN	Prosthion to Inion
PRBR	Prosthion to Bregma
PRRH	Prosthion to Rhinion
PROB	Prosthion to Zygoorbitale
INOB	Inion to Zygoorbitale
ZMOB	Zygomaxillare to Zygoorbitale
ZMPG	Zygomaxillare to Postglenoid
BIPG	Bi-Postglenoid Breadth (centers of process tips)
MAXW	Maximum Vault Width (on temporal dorsal to porion or zygomatic arch)
FACH	Face Height (top of brow ridge to alveolar margin; cranium in alveolar plane)
BIZY	Maximum Bi-Zygomatic Breadth
TMIN	Minimum Temporal Line Width (between medialmost edges; if sagittal crest exists, defined as 1 mm)
PORB	Minimum Postorbital Width
BIOR	Bi-Orbital Breadth (taken on lateral margin of frontal/zygoma; near Fronto-malar temporale)
INOR	Minimum Interorbital Distance (close to Bi-Dacryon; but often not as deep into orbit)
ORBH	Orbit Height (taken near center of orbit)
ORBW	Orbit Width (taken near center of orbit)
SUPO	Supraorbital Torus Thickness (taken near center of orbit; maximum away from notch)
FORW	Maximum Foramen Magnum Width
FORL	Foramen Magnum Length (Basion to Opisthion)
NASW	Maximum Nasal Aperture Width
NASL	Maximum Nasal Aperture Length (Rhinion to Nasospinale)
BMEU	Breadth across upper molars (on alveolar margin between M1 & M2)
I1MU	Maximum breadth across upper I1 (Chord across 2 incisors near tips)
I1AU	Breadth across upper I1 at alveoli (chord across 2 incisors at alveolar margin)
M3IU	Upper I1 to M3 (I1 incisal edge to M3 distal face)
M3MU	Upper M1 to M3 (M1 mesial face to M3 distal face)
ALWU	Width of maxillary alveolar process (near middle of M2)
PDEP	Depth of palate (near middle of M2; from alveolar margin projected to midline)
AFAC	Facial angle (Approximate angle of alveolar margin and Glabella to Prosthion chord)
IDCO	Infradentale to Condylion (midpoint of condyle)
SYML	Symphyseal Length (Infradentale to Gnathion)
PLAL	Alveolar Planum Length (Infradentale to Inferior Endpoint of planum alveolare)
GNAL	Gnathion to Inferior Endpoint of PLAL
GNGO	Gnathion to Gonion
RAML	Length (M-D) of mandibular ramus (minimum anterior–posterior [=mesial-distal] length of ramus above alveolar plane and below incisura; often called “width”)
CORH	Height of coronoid process (with mandible resting on flat support; maximum height above support of coronoid process)
BJD3	Buccal corpus depth below m3 (depth from alveolar margin in middle of m3 to inferior border of corpus)
BJD4	Buccal corpus depth below p4 (depth from alveolar margin in middle of p4 to inferior border of corpus)
ALWL	Width of mandibular alveolar process (near middle of m2)
M3IL	Lower i1 to m3 (i1 incisal edge to m3 distal end)
I1AL	Breadth across lower i1 at alveoli (chord across 2 incisors at alveolar margin)
I1ML	Maximum breadth across lower i1 (chord across 2 incisors near tips)
ARAM	Ramus-corpus angle (approximate angle of corpus inferior margin and [upper] posterior margin of ramus at gonion)
ASYM	Symphyseal angle (approximate angle of corpus inferior margin and anterior face of symphysis at gnathion)

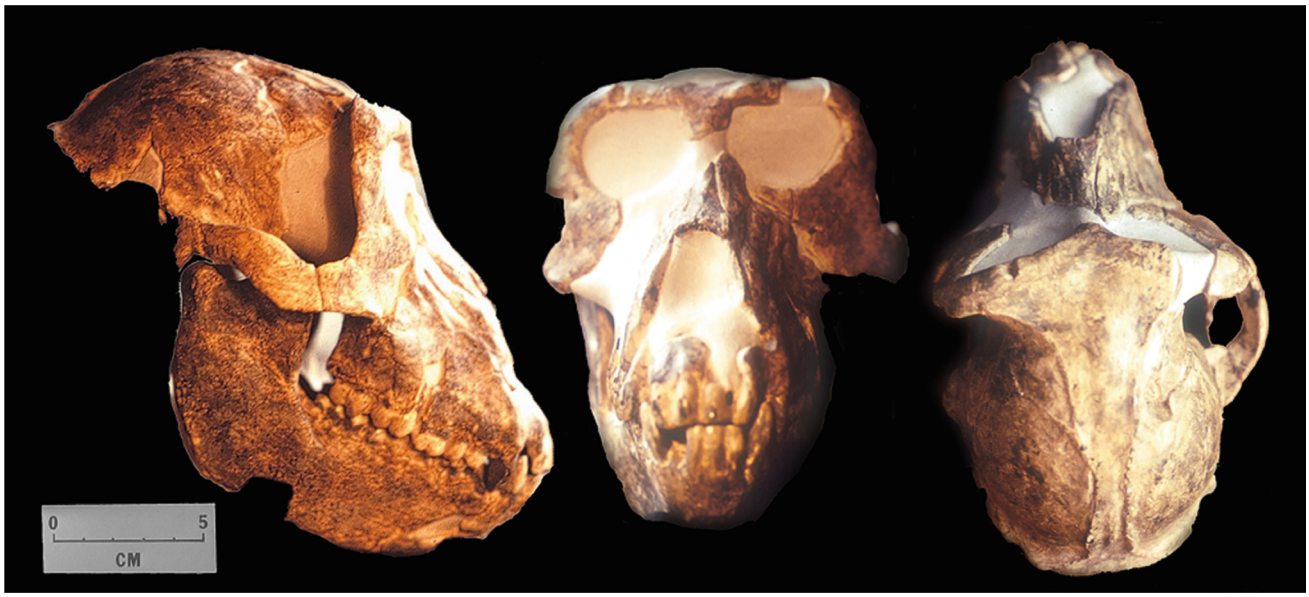

Fig. 16.4 *Paradolichopithecus arvernensis*, cast of Battetta (1969) reconstruction of FSL 41336 Senèze female holotype skull. Left to right: left lateral (Frankfurt plane), frontal and dorsal (occlusal plane) views, photos by F.S. Szalay

inferior margin, producing a "D" shape (Figs. 16.4 and 16.11). The nasal bones are smoothly curved and not raised. Several infraorbital foramina lead into shallow grooves on the maxilla, which shows no sign of a fossa or other excavation. The nasal aperture is oval in anterior view, with maximum width about halfway down, but the inferior portion is damaged. The maxillary root of the zygomatic arch arises above the distal part of M3. The arch itself is very deep, giving the face great lateral robusticity. As Simons (1970) illustrated and discussed, the overall shape in lateral view is similar to that in males of several macaque species (e.g., *M. nemestrina* or *M. nigra*), whose longer faces compare better to *Paradolichopithecus* of both sexes than those of female macaques.

The palate is poorly preserved, but there is a slight shallowing mesially and not much elongation due to the small canines. The toothrow widens slightly from M3 to M2, then narrows mesially to C, as in female macaques but unlike females of *Papio*, *Mandrillus*, *Soromandrillus* or *Dinopithecus*, which are of comparable palate length but narrower and more straight-sided.

FSL 41336 has a shallow supraorbital notch on the right with a slight projection medially; the left side is damaged and unclear (Fig. 16.6). Based on the analysis of a CT scan by Nishimura et al. (2014; Fig. 16.12 here), an inferior concha likely descended from the superior portion of the nasal cavity, which would have separated a large inferior meatus from the main portion of the nasal cavity at the level of M1 to mesial M2. There is no indication of a maxillary sinus, a conservative trait shared with most extant cercopithecoids excluding macaques.

Calvaria. Behind the tall but not protruding supraorbital tori, there is a small ophryonic depression. The temporal lines arise near the lateral ends of the tori and turn fairly sharply medially before curving posteriorly well medial to the postorbital constriction. The lines converge to a closest approach (12 mm) on the posterior parietals before diverging slightly and eventually meeting the strong nuchal crest, which turns neither up nor down at inion but remains level. This pattern is most similar to that seen in male macaques. The occipital planum is fairly smooth and angled from the nuchal crest to the foramen magnum. The postglenoid process is robust and leans anteriorly only slightly; the mandibular fossa is wide.

Mandible. The Senèze mandible is well preserved. The anterior symphyseal surface is robust, with relatively strong muscle scars bounding the smooth midline region. The scars are less posterolateral than in female *Papio* or *Mandrillus* mandibles of nearly similar size, but more pronounced than in those of large female macaques (which are far smaller overall). Large male macaques (e.g., *M. nemestrina leonina*, AMNH-M 11090) are perhaps most similar in shape. The planum alveolare is long, the superior torus slight and the inferior torus barely present. There is a slight corpus fossa (really just a shallowing) below the p4-m1 contact, also as in male macaques but not female papioninans, which usually have significant fossa development (see e.g., Gilbert 2013). Corpus depth remains constant from m1 to m3 and beyond, the margin curves smoothly through gonion and up the distal edge of the ramus to the condyle. A strong buccinator groove precedes the anterior edge of the ramus, which rises subvertically and thickens slightly below the coronoid. The

Fig. 16.5 *Paradolichopithecus arvernensis*, FSL 41336, Senèze holotype skull, neurocranial element. Top to bottom: left lateral and dorsal views (near Frankfurt plane)

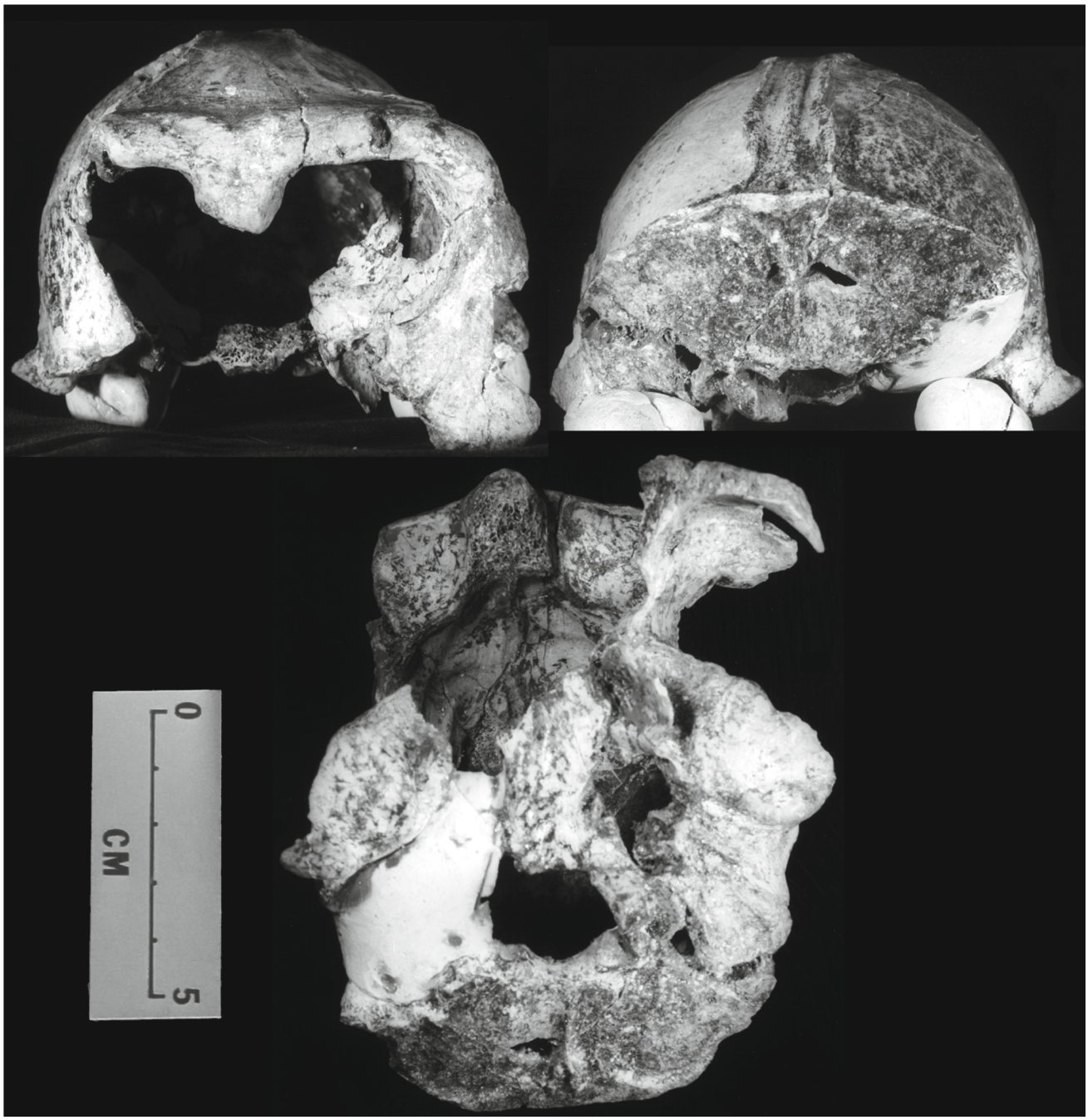

Fig. 16.6 *Paradolichopithecus arvernensis*, FSL 41336, Senèze holotype skull, neurocranial element in frontal (top left), occipital (top right) and basal (below) views (near Frankfurt plane)

Fig. 16.7 *Paradolichopithecus arvernensis*, FSL 41336, Senèze holotype skull, right maxilla with separated partial right premaxillary fragment and isolated I1 attached, in lateral (left) and occlusal (right) views (occlusal plane)

posterior slope of the coronoid is nearly linear, and the notch is acute but restricted. The ramus is angled slightly posteriorly relative to the corpus, most comparable to that of female *M. tonkeana hecki* (e.g., AMNH-M 152897) or *Mandrillus sphinx* (e.g., AMNH-M 89357), rather than "leaning" farther posteriorly as in female *Papio* spp. or male macaques, or being nearly vertical as in smaller papioninans or some female macaques (e.g., *M. thibetana*, AMNH-M 83994).

Implications for Paleoenvironment and Relative Age

The two primate taxa known from Senèze provide only slight information about the local environment or age of the site. *Macaca sylvanus* is known across much of Europe in small numbers throughout the Pliocene and Pleistocene. Based on the extant populations of the Maghreb, the species often feeds and travels on the ground in open to mixed woodland and into grassland but sleeps in trees (Fooden 2007; Rowe and Myers 2016). Environments are variable, often wet and cold (even snowy) in winter, with warm and dry summers. Its postcranium is moderately adapted to terrestriality, among the most cursorial of macaques. *Paradolichopithecus arvernensis* is known by postcrania from Grăunceanu and Vatera which are similar to those of *Papio* and *Mandrillus* (Ting et al. 2004, Delson et al. in preparation). They suggest a high degree of terrestriality, perhaps in open terrain to woodland.

European macaques do not yet provide any direct indication of geological age. Delson (1980; Szalay and Delson 1979) suggested that several chronosubspecies could eventually be distinguished, but later studies (e.g., Alba et al. 2008, 2011) have not confirmed his proposal; further analysis is in progress. Delson and Plopsor (1975) and Aguirre and Soto (1978) suggested that *Paradolichopithecus arvernensis* might serve as a marker for the beginning of the Calabrian Stage, then recognized as the base of the Pleistocene. Current assessments of age for localities including the genus (listed above) in fact reveal a range from at least 4 Ma to 2 Ma, with no known specimens in Calabrian-age deposits. Detailed analysis is still ongoing, but the Senèze population appears to be slightly larger than that from Grăunceanu in terms of cranial size, which led to previous suggestions that female crania (then known only from Senèze) were little smaller than males (known from

Fig. 16.8 *Paradolichopithecus arvernensis*, FSL 41336, Senèze holotype skull, mandible in two pieces loosely attached in occlusal view (occlusal plane)

Grăunceanu) and thus that sexual dimorphism was less than expected in a cercopithecine of this size. The subadult female Dafnero cranium is crushed bilaterally and distorted, but it appears similar in size to the Senèze specimen. It may be that Senèze is younger than Grăunceanu (whose precise age is still unknown, see Terhune et al. 2020), given that the still older populations termed *Paradolichopithecus* sp. appear even smaller.

Recently Benammi et al. (2020) have proposed on the basis of magnetostratigraphy that Dafnero, faunally similar to Vatera (and Grăunceanu), might date to ca 2.3 Ma. They studied two neighboring sections, both of which contained a normal magnetozone between reversed intervals, with the faunal level near the bottom of each section. They estimated the age of the fauna between 2.5 and 2.0 Ma and thus correlated the normal magnetozone with either the Olduvai or the "Réunion" (now Feni) subchron. They compared the thickness of the normal magnetozone to the length of those two normal intervals to approximate the sedimentation rate for each correlation hypothesis and in turn to estimate the duration of the interval between the base of the normal and the fossiliferous level. This yielded an estimated age of 2.4 Ma if the normal correlated to the Olduvai and 2.2 Ma if it was the Feni (based on a 20 kyr duration of the latter).

However, there are a number of problems in their approach. First, in the two magnetostratigraphic sections studied, there are only 2 normal samples over a span of 5–10 m, and the stratigraphic length of the normal was calculated by placing the estimated end points almost randomly between the normal samples and the nearest reversed sample (rather than midway between the nearest sample levels as is usually done). Moreover, the sampling interval was not tight enough to delineate the polarity zones that closely; on average there are several meters between samples. It is not clear if the normal or reversed zones were significantly shorter or longer than estimated. Given the dates for Senèze in Nomade et al. (2014), which they cited, the normal is most likely to be the Feni, not the Olduvai. But Benammi et al. (2020) used an older age range for the Feni of 2.148–2.128 Ma, rather than the current 2.14–2.116 Ma (26 not 20 kyr; see Channell et al. 2020). Therefore, the age can only be estimated as older than Feni and younger than the Gauss-Matuyama boundary, i.e., 2.58–2.14 Ma. A date between 2.6 and 2.2 Ma is the most reasonable approximation, perhaps older in that range as the fossils come from low in the section. The Senèze specimen of *Paradolichopithecus arvernensis*, dated between 2.2 and 2.1 Ma (Delson et al. 2024) may be one of the youngest known representatives of the genus.

Discussion

There are two major questions about *Paradolichopithecus* which have been raised in the literature: distinction from *Procynocephalus* and affinity to Papionina or Macacina. Delson and colleagues (e.g., Delson and Plopsor 1975; Szalay and Delson 1979; Delson et al. 2000, 2014; Delson and Frost 2004) agreed with previous work by Vogel (1966, 1968), Jolly (1967) and Simons (1970) in arguing for morphological similarity to *Macaca*. They also opted to retain the two Plio-Pleistocene forms as distinct genera, pending the possibility of more direct comparison. Maschenko (1994, 2005) suggested that *Paradolichopithecus* (especially "*P.*" *sushkini*) was instead close to or even congeneric with *Papio*. Kostopoulos et al. (2018) also suggested a close relationship with *Papio* and further argued that *Paradolichopithecus* could be included in *Procynocephalus* as there were few if any features that separated the two genera. Le Maître et al. (2023) supported the possibility that *Paradolichopithecus* (or *Procynocephalus*) aligned more closely with Papionina than Macacina based on morphology of the bony labyrinth.

Fig. 16.9 *Paradolichopithecus arvernensis*, FSL 41336, Senèze holotype skull, left mandibular segment in lateral above internal views (occlusal plane, interval view photographically reversed); left c-m_3 inset at 1.3 × main scale

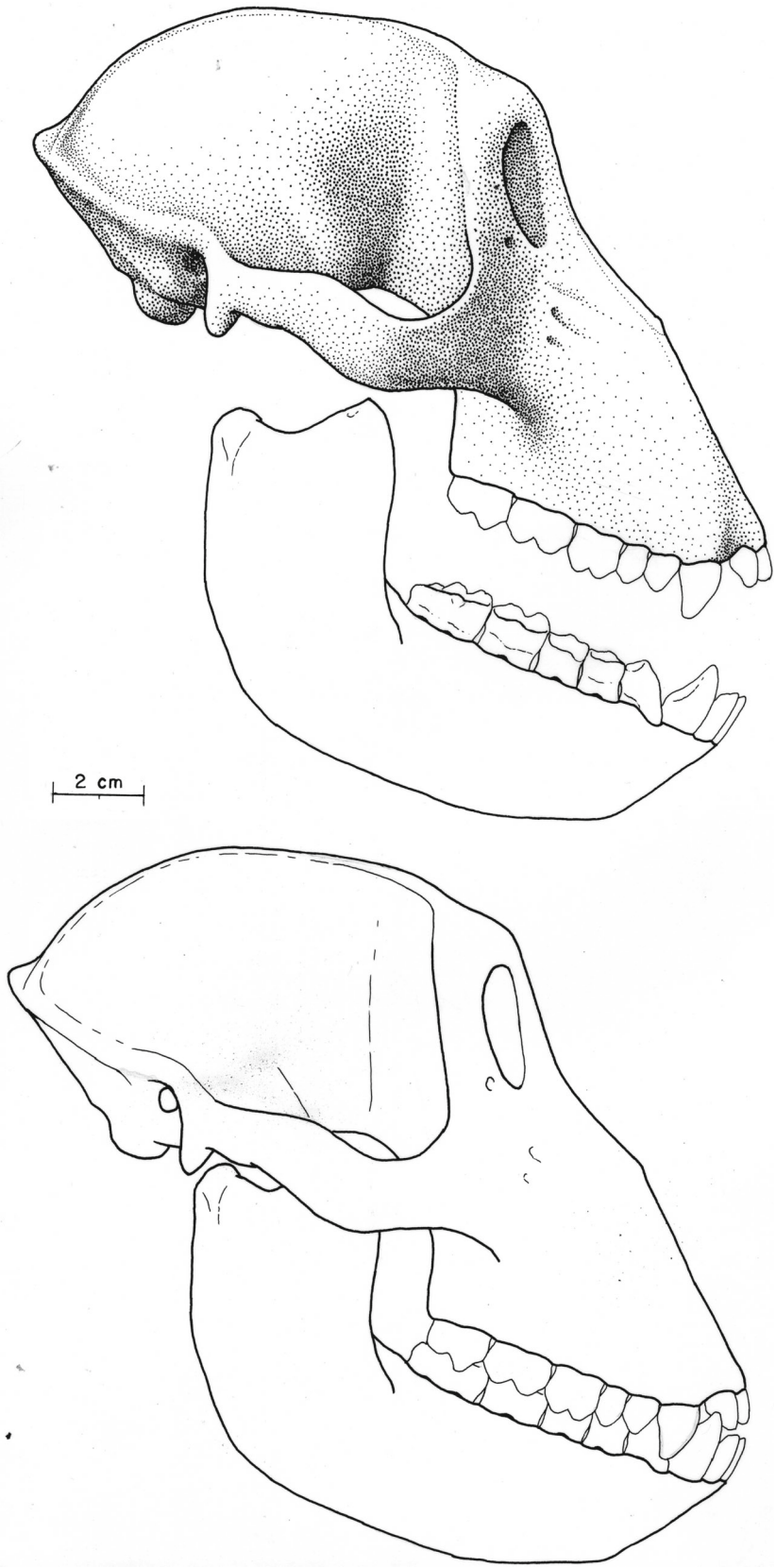

Fig. 16.10 *Paradolichopithecus arvernensis*, FSL 41336, Senèze holotype skull, right lateral drawings in Frankfurt plane: cranium and mandible separated above the two elements in occlusion, artwork by B. Akerbergs

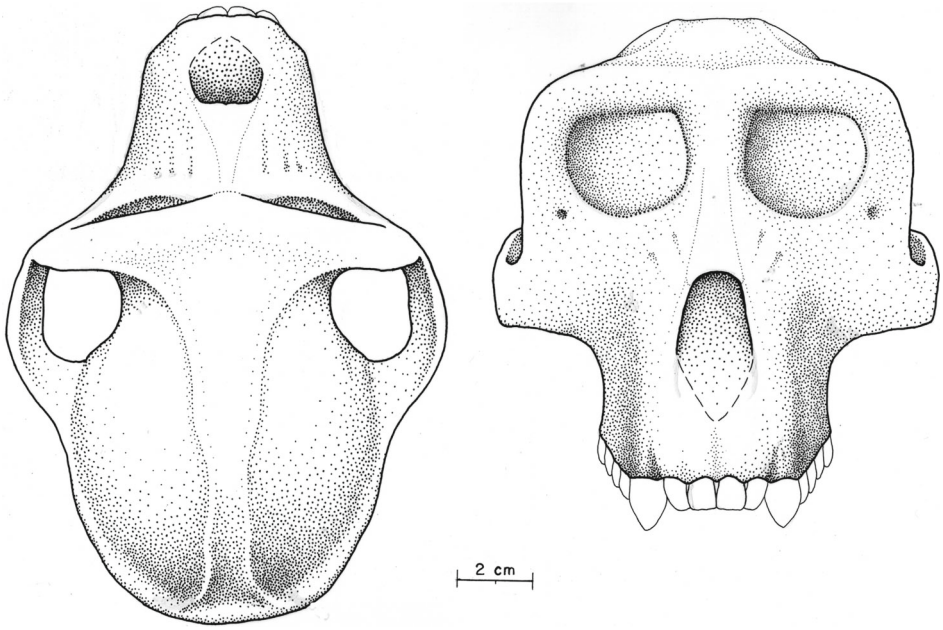

Fig. 16.11 *Paradolichopithecus arvernensis*, FSL 41336, Senèze holotype skull, drawings in Frankfurt plane: cranium in dorsal (left) and frontal (right) views, artwork by B. Akerbergs

Are Paradolichopithecus *and* Procynocephalus *synonymous or distinct genera?*

Kostopoulos et al. (2018: 188–189) listed a number of features they claimed were shared by *Paradolichopithecus* and *Procynocephalus*:

(a) similar size and body mass;
(b) similar dental morphology, low fourth premolar to first molar area ratio and a strong molar flare;
(c) females with weak to moderate anteorbital drop (comparison between DFN3-150, UCBL-FSL 41336, and PIN 3120–523 of *Paradolichopithecus* and the partial face of female *Pro. subhimalayanus* illustrated by Szalay and Delson (1979: Fig. 181A);
(d) premaxillary bones marginally reaching nasal bones;
(e) females with a smoothly rounded anterior muzzle traveling upward towards the nasion in a gentle curve (comparison based on the same specimens as (c); more vertical in male *Paradolichopithecus*);
(f) females with weak to absent maxillary fossae and weak to moderate but always present (n = 7) fossae of the mandibular corpus;
(g) narrow parabolic upper and lower toothrows with parallel molar series;
(h) small (compared to I2) and non-shovel shaped first incisors;
(i) a gradually descending capitulum of the distal humerus (shared between *Pro. wimani* and *Paradolichopithecus* from Vatera, Greece; e.g., van der Geer and Sondaar 2002);
(j) a protruding (in dorsal view) lateral suspensory facet for the fibular malleolus of the talus and parallel trochlea tali (shared between *Pro. wimani* and *Paradolichopithecus* from Valea Grăunceanului, Romania and Vatera, Greece; e.g., van der Geer and Sondaar (2002) and Sondaar et al. (2006);
(k) a narrow coronoid process of the proximal ulna (shared between *Pro. wimani* and *Par. geticus*; compare Fig. 182f and 186f in Szalay and Delson (1979) in relation to Fleagle and McGraw (2002: Fig. 10).

Of these 11 points, restricting the comparison to *Paradolichopithecus arvernensis*, *Procynocephalus wimani* and *Pro. subhimalayanus* (see Fig. 16.13), a, b, d and probably g and h are just a matter of similar large size (equivalent to *Papio* and other large genera unrelated to *Mandrillus*); *c* may be correct but linked to relationship with *Macaca*, although breakage mostly prevents observation of the anteorbital region in NHMUK-P M37157; *e* is untrue, *Pro. subhimalayanus* has a more flattened muzzle dorsum, confirmed by a CT scan which shows that this shape is not due to crushing; *f* again is expected for relatives of *Macaca*, and the mandibular corpus fossa is not as extensive as suggested (see above); *i*, *j* and *k* are correct, due to similar locomotor adaptation (a Grăunceanu humerus, which is less

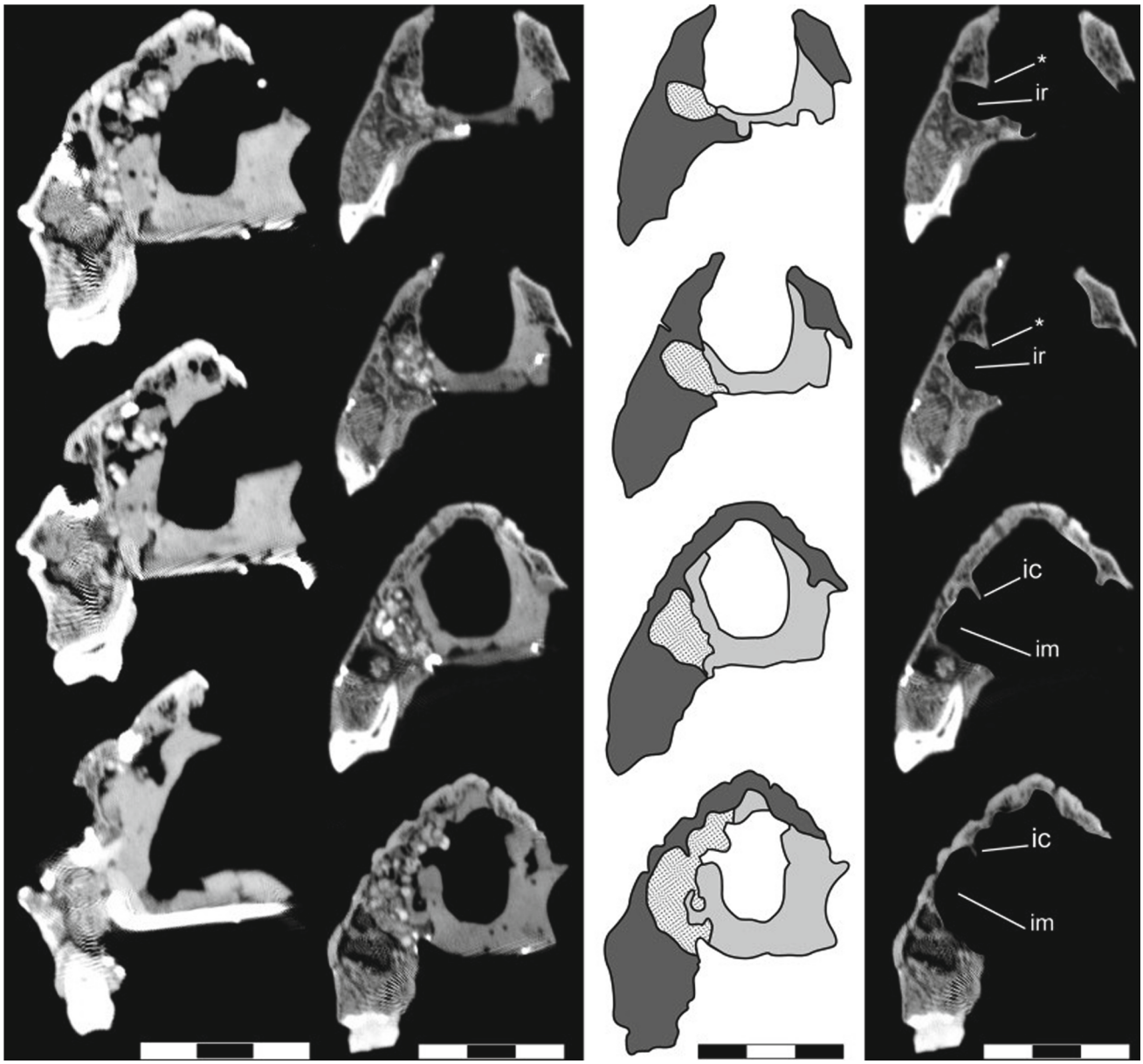

Fig. 16.12 *Paradolichopithecus arvernensis*, FSL 41336, Senèze holotype skull, coronal CT scan slices from Nishimura et al. (2009), with permission: left column, top to bottom, slices through mesial, middle and distal regions of M3; second column, top to bottom, slices through M1, M1-2 contact area, M2, M2-3 contact area; third column, top to bottom, interpretive schematic drawings of previous slices; right column, top to bottom, images virtually excluding the bony structure. The scales are in centimeters. The areas filled in dark gray, light gray, and dots on the schematic drawings indicate bone, cement or plaster, and matrix, respectively. At the level of M1 and M1–2 contact on the right (left on the image), a small inferior recess (ir) accompanies a thick bony ridge projecting inferiorly and medially (*). At the level of M2 and M2–3 contact, a thin basal portion of the inferior concha (ic) descends from the superior portion of the muzzle, and the inferior meatus (im) expands laterally and superiorly to occupy a large area of the nasal cavity. At the level of mesial M3, the inferior concha (ic) can be observed in the superior portion of the muzzle and the maxillary body faces just the inferior meatus. The nasolacrimal canal probably extended anteriorly through the lateral-superior region (**, area in white) of the muzzle at the level of middle M3, opening towards the inferior meatus (*) at the level of mesial M3. The inferior concha can be observed from the middle portion of the maxillary body at the level of distal M3 and the superior portion of the body faces the middle meatus. The medial bony wall (bw) separates the maxillary body continuously from the middle meatus of the nasal cavity

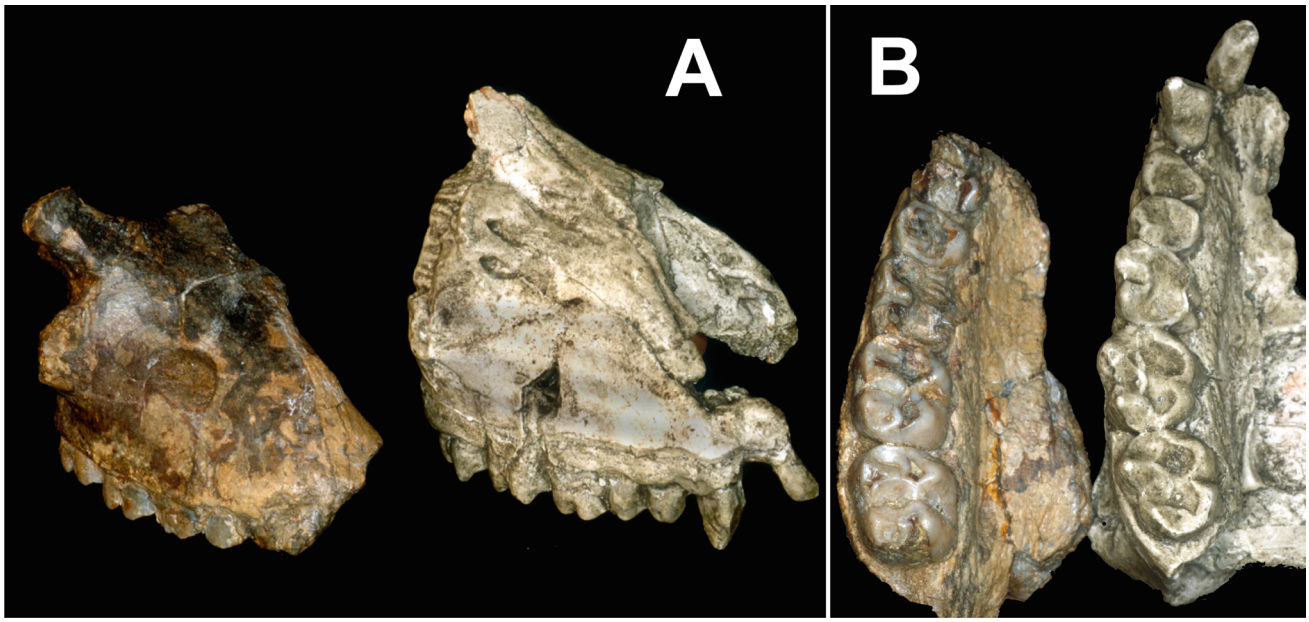

Fig. 16.13 Maxillae of female large cercopithecines: right, FSL 41336, the Senèze holotype of *Paradolichopithecus arvernensis* (cast) and left, NHMUK-P M37157, the Siwalik holotype of *Procynocephalus subhimalayanus*; (**A**) right lateral view, slightly oblique, showing difference in elevation of muzzle dorsum; (**B**) occlusal view, showing similarity in size

distorted, is illustrated in Szalay and Delson 1979 and in Sondaar et al. 2006; *Pro. wimani* [illustrated by Teilhard de Chardin 1938] and Vatera are similar, but there is no talus known from Grăunceanu).

Kostopoulos et al. (2018) also noted the presence of *Paradolichopithecus* in China, but in fact the generic identity of "*P.*" *gansuensis* is moot. Qiu et al. (2004, p. 170), in part following Trofimov (1977), suggested that the cheek teeth of *Paradolichopithecus* are more lophodont than those of *Procynocephalus* and the distal margin of the M3 is more rounded, with a larger fovea. These distinctions are not supported by an examination of all available *Paradolichopithecus arvernensis*, which show some variability in the "crestiness" of the lower molars especially. Dental features do not seem to distinguish between the two genera, and thus the Longdan species is only questionably indicated here as possibly *Paradolichopithecus*. Kostopoulos et al. (2018, p. 188) further suggested that the Dafnero specimen could be included just as easily in *Procynocephalus wimani* due to shared morphology, such as "weak-moderate anteorbital drop", but that feature is not visible in the holotype maxilla of *P. wimani* (see Nishimura et al. 2014).

Thus, all the points where the two genera are similar can be explained by comparable size, linkage to *Macaca* and/or locomotor adaptation. One character does appear to separate the genera, namely the shape of the muzzle dorsum, which is more elevated and "peaked" in *Paradolichopithecus arvernensis* but relatively flattened in *Procynocephalus subhimalayanus* (Fig. 16.13 A), although not at all as much so as in large Papionina. Pending further analysis and additional material of *Procynocephalus*, the two genera should be kept distinct.

Macacina or Papionina

Determining the subtribal allocation of *Paradolichopithecus*, whether Macacina or Papionina, is also fraught. Maschenko (1994, 2005) discussed the large primate from Kuruksay as *Papio* (*Paradolichopithecus*) *sushkini* in some places and *Papio sushkini* in others. It is not clear if he meant to use *Paradolichopithecus* as a subgenus or was merely indicating the "original" name parenthetically. He also mentioned *Paradolichopithecus arvernensis* without employing *Papio* as part of the name.

In a summary of his views, Maschenko (2005, pp. 111–112) wrote: "*Papio sushkini* … is similar to recent *Papio* in morphology of the infraorbital foramina, ratio of lengths of the facial and cranial parts of the skull, the short and robust alveolar process of the upper jaw, the large anteroposterior diameter of foramen magnum, the shape of the nasal bones, position of the fossa glandula lacrimalis (only on os lacrimale), shape of the cecal foramen, morphology of the CP3 complex molar morphology, and relation of lengths of the premolar and molar tooth rows. Specialization of *Papio sushkini* in comparison with modern representatives of the genus is found in a greater robustness of molars relative to premolars, greater enamel thickness, greater length of the zygomatic arch relative to total length of the skull, and a more robust M^3 in comparison with M^2."

Once again, most of these similarities are linked to the large size of the Eurasian fossils. Maschenko (1994, 2005) did not mention the anteorbital drop characterizing *Papio* or its lack in the fossils, which may be the most diagnostic distinction of *Macaca* and *Paradolichopithecus* from *Papio*.

Kostopoulos et al. (2018) also plotted the P4/M1 area ratio, using a much smaller sample and both sides of the jaw for fossil specimens. They found that the *Paradolichopithecus* box overlapped the P-L–T range but only the whisker of *Macaca*, while the *Paradolichopithecus* upper whisker overlapped the *Macaca* box and the lower end of the C-M range. From this pattern, they suggested another similarity to Papionina rather than Macacina, but their results are vitiated with the larger samples used here (Fig. 16.2, see above).

As noted previously, Le Maître et al. (2023) analyzed the inner ear bony labyrinth morphology of the Dafnero specimen and other cercopithecines. They concluded with some hesitancy that *Paradolichopithecus* showed similarities to Cercopithecini and Papionina, but not to macaques. They suggested that *Paradolichopithecus* might be a stem papioninan or perhaps a basal papionin closer to Papionina than to *Macaca*. The data they presented do not strongly support these conclusions.

In their introductory remarks, Le Maître et al. (2023, p. 210), reported the disagreement between those who considered *Paradolichopithecus* (and *Procynocephalus*) macaque-related and those who "propose closer phylogenetic affinities with the African baboons". The first author they cited in the latter group is Jolly (1967), who in fact clearly linked both taxa with Asian macaques (p. 45). They may have been confused by his broad use of the term "baboon", by which he meant terrestrial cercopithecines (and possibly colobines), usually large and long-faced.

Le Maître et al. (2023, p. 218) studied both labyrinths of the Dafnero cranium, noting that the left one was undistorted, while the right was damaged and somewhat distorted. Overall shape was most similar to those of *Erythrocebus patas* and *Mandrillus sphinx*. Some features were similar to those seen in Papionina, but some also occurred with Macacina. Typicality probabilities determined from their bgPC analysis indicated that the left labyrinth was most likely to be a cercopithecin, while the (distorted) right grouped with papioninans; linkage to macaques was low (p. 224).

In a plot of regression score vs. log centroid size (Fig. 16.3, p. 220), macaques fell mostly below the regression line for the whole sample, along with some *Chlorocebus* and two of the three *E. patas*, with the Dafnero fossil falling near one of the latter, on the Cercopithecini line. Few papioninans fell below the overall line. Plots of the first four PCs from a standard PCA (Fig. 16.4, p. 221) revealed that the fossil has no clear affinities with any clade but was said to weakly group with Papionina (p. 223).

Three neighbor-joining cluster analyses based on Euclidean distances (p. 225) include the Dafnero specimen but do not capture known phylogenetic relationships (as they mentioned on p. 226). The fossil often links with *Mandrillus sphinx*, but also with *Macaca nigra* and a *Papio*; and centroid size (allometry) is important when included. None of the three tribal-group taxa (Macacina, Papionina and Cercopithecini) is consistently monophyletic; this does not lead to much faith in the systematic placement of the Dafnero fossil. A discussion of phylogenetic signal across these features also finds only a weak signal and suggestions of hesitancy (p. 227): "interpreting these results is tricky, because the null hypothesis of no pattern of similarity among relatives is very unlikely to be true in any biological organism."

Overall, the discussion is rather convoluted, noting some links but ignoring others. Similarities to macaques are mostly suggested to be ancestral retentions from a basal papionin or cercopithecine ancestry (p. 228). Le Maître et al. (2023, p. 229) wrote: "we can not exclude that the shape affinities of *Paradolichopithecus* with the baboon-related clade are the result of a parallel evolution for large, terrestrial species that would arise from a common allometric pattern across all cercopithecines." They noted (p. 230) that similarities of cranial shape between young *Paradolichopithecus* (i.e., Dafnero) and *Macaca* could be related to similar growth trajectories in all papionins, but they make no mention of adult similarity. In sum, they conclude that *Paradolichopithecus* is phylogenetically unrelated to macaques but either a papioninan or a basal papionin closer to papioninans. They wrote (p. 231): "Our findings do not provide a clear answer to the taxonomic classification of *Paradolichopithecus*, though the traditional hypothesis of a *Paradolichopithecus*–Macacina relationship appears to be the least supported."

Two incompletely published analyses presented arguments for the opposite view, namely that *Paradolichopithecus* is a phylogenetic sister to *Macaca*. Delson and Frost (2004) mentioned the results of a 3D geometric morphometric analysis of the face which linked *Paradolichopithecus* from Senèze (and Grăunceanu) to macaques rather than *Papio* when allometry (centroid size) was included; the details of this study were presented in the talk and will be included in Delson et al. (in preparation). An analysis of cranial landmarks placed the *Paradolichopithecus* specimens within the *Macaca* scatter but also showed some overlap with *Papio*. However, analyses of the lateral muzzle profile and the transverse curvature of the dorsal rostrum more clearly placed *Paradolichopithecus* with *Macaca* to the exclusion of *Papio*. Delson and Frost (2004) also noted that *Paradolichopithecus* had relatively small I1 area compared to M1 area (this is indicated in Table 16.2), but this pattern

might in part be related to greater wear of the *Paradolichopithecus* incisors in older individuals.

O'Shea et al. (2016) presented preliminary results of a cladistic analysis also placing *Paradolichopithecus* with macaques. Details will be included in Delson et al. (in preparation), but their poster listed a number of synapomorphies with *Macaca*: intermediate pinching of the anterior temporal lines (in females); tympanic unfused and moderately separated from the postglenoid process (both sexes); maxillary fossa and maxillary ridge absent (in males); and glabella moderately prominent (both sexes). This resulted in a macacinan clade sister to Papionina (crown *Papio-Lophocebus-Theropithecus* and *Cercocebus-Mandrillus* groups plus several stem taxa), with some *Parapapio* and the outgroups "*Parapapio*" *lothagamensis* and *Victoriapithecus macinnesi* outside the crown.

For the moment, at least, it appears that a *Paradolichopithecus-Macaca* relationship is better supported than one linking the large Eurasian fossils with *Papio* or Papionina as a whole.

Summary

Two cercopithecid fossils are known from Senèze. A partial ulna represents cf. *Macaca sylvanus*. The holotype of *Paradolichopithecus arvernensis* (Depéret, 1928) is a nearly complete female skull. A brief history of research on *Paradolichopithecus* is provided. Emended diagnoses of both *Paradolichopithecus* and *P. arvernensis* are presented, with comparisons to other papionin genera. The Senèze skull is described in detail. *Macaca* and *Paradolichopithecus* are postcranially adapted to a partly or fully terrestrial habitus (based on material from other sites); this supports a relatively open wooded landscape around the Senèze maar. *Paradolichopithecus arvernensis* from Senèze may be one of the youngest known occurrence of the genus, at 2.2–2.1 Ma. The Grăunceanu sample is possibly somewhat older based on a slightly smaller size. The crushed subadult female from Dafnero appears similar in size, and a reassessment of the reported paleomagnetic data suggests an age between 2.58 and 2.2 Ma.

Two questions regarding the systematics of *Paradolichopithecus* are actively discussed: is it a synonym of *Procynocephalus* and is it more closely related to *Macaca* or *Papio*? Most features shared by the two Eurasian fossil genera are based on large size and terrestrial locomotor adaptation, although they differ in the shape of the muzzle dorsum; thus both genera are retained as distinct. Similarly, features suggesting a link between *Paradolichopithecus* and *Papio* (or other papioninans) mainly appear related to shared large size. Claimed distinctions or links related to the P4/M1 area ratio and the shape of the bony labyrinth do not stand up to scrutiny. Unpublished 3D geometric morphometric and cladistic analyses of the cranium do support a *Paradolichopithecus-Macaca* relationship.

Acknowledgments I thank Prof. L. David and Drs. M. Faure, C. Guérin, P. Mein, A. Prieur, E. Robert (UCB-Lyon 1) and J. Hürzeler (NMB) for facilitating my access to the Senèze fossil primates over many decades. I thank many curators and collection managers/associates of the Department of Mammalogy, American Museum of Natural History, for allowing me to make use of their incomparable collection of cercopithecid and other primates over an even longer period. Many other curators of fossil and extant primate collections across Europe permitted me to study specimens in their care. My travel to Senèze and to Lyon and other collections was supported, in part, by research grants from many sources, including Columbia University, the Leakey Foundation, the National Science Foundation (grants BCS-0083166 and -0104781), the National Geographic Society (grants 944, 7050-01 and 7434-03), the PSC-CUNY faculty research program (awards 11152, 6-69381, 6-64333, 6-65407, 63528-32. 64542-33, 65509-34, 66578-35. 67356-36 and 68016-37) and the Wenner-Gren Foundation for Anthropological Research (grant no. 2810).

I acknowledge Ms. Biruta Ackerbergs for her drawings of the Senèze cranium and mandible (from casts), originally made for inclusion in Szalay and Delson (1979). I thank Drs. Fred Szalay and Takeshi Nishimura for permission to use their images in Figs. 16.2 and 16.10. I thank Dr. Martine Faure for locating and showing me Depéret's (1928) article and for writing the résumé in French.

I thank Julia L. Arenson, Dr. Martine Faure and Dagmawit Abebe Getahun for comments on an early version of this manuscript. I thank Dr. Eric J. Sargis and especially reviewers Drs. David Alba, Stephen Frost and Christopher Gilbert for their helpful suggestions. All of these have improved the manuscript significantly.

References

Aguirre, E., & Soto, E. (1974). Nuevo fósil de Cercopitécido en el Pleistoceno inferior de Puebla de Valverde (Teruel). *Estudios Geológicos, 30*, 213–217.

Aguirre, E., & Soto, E. (1978). *Paradolichopithecus* in La Puebla de Valverde, Spain: Cercopithecoidea in European Neogene stratigraphy. *Journal of Human Evolution, 7*, 559–565.

Alba, D. M., Moyà-Solà, S., Madurell, J., & Aurell, J. (2008). Dentognathic remains of *Macaca* (Primates, Cercopithecidae) from the late early Pleistocene of Terrassa (Catalonia, Spain). *Journal of Human Evolution, 55*, 1160–1163.

Alba, D. M., Carlos Calero, J. A., Mancheño, M. Á., Montoya, P., Morales, J., & Rook, L. (2011). Fossil remains of *Macaca sylvanus florentina* (Cocchi, 1872) (Primates, Cercopithecidae) from the Early Pleistocene of Quibas (Murcia, Spain). *Journal of Human Evolution, 61*, 703–718.

Battetta, J. (1969). Compte rendu du remaniement de la reconstitution du crâne de *Dolichopithecus arvernensis* Depéret, type. *Bulletin mensuel de la Société Linnéenne de Lyon, 38ème année*, 279–284.

Benammi, M., Aidona, E., Merceron, G., Koufos, G.D. & Kostopoulos, D.S. (2020). Magnetostratigraphy and chronology of the Lower Pleistocene primate bearing Dafnero fossil site, N. Greece. *Quaternary, 3*, 22 [16 pp.]; https://doi.org/10.3390/quat3030022.

Burnett, G. T. (1828). Illustrations of the Manupeda or apes and their allies: Being the arrangement of the Quadrumana or

Anthropomorphous beasts indicated in the outline. *Quarterly Journal of Science, Literature and Art, 26*, 300–330.

Channell, J. E. T., Singer, B. S., & Jicha, B. R. (2020). Timing of Quaternary geomagnetic reversals and excursions in volcanic and sedimentary archives. *Quaternary Science Reviews, 228*, 106114.

Crégut-Bonnoure, E., Guérin, C., Argant, A., Argant, J., Debard, E., & Delson, E., et al. (2024). Biochronology of the Senèze faunal assemblage. In E. Delson, M. Faure & C. Guérin (Eds.), *Senèze: Life in Central France two million years ago. Paleontology, geochronology, stratigraphy and taphonomy* (pp. 633–652). Cham (Switzerland): Springer.

Delson, E. (1971). Estudio preliminar de unos restos de simios pliocenicos procedentes de "Cova Bonica" (Gava) (Prov. Barcelona). *Acta Geológica Hispánica, 6*, 54–57.

Delson, E. (1974). Preliminary review of cercopithecid distribution in the circum-Mediterranean region. *Mémoires du Bureau de Recherches Géologiques et Minières, 78*, 131–135.

Delson, E. (1975). Evolutionary history of the Cercopithecidae. *Contributions to Primatology, 5*, 167–217.

Delson, E. (1977). Catarrhine phylogeny and classification: Principles, methods and comments. *Journal of Human Evolution, 6*, 433–459.

Delson, E. (1980). Fossil macaques, phyletic relationships and a scenario of deployment. In D. G. Lindburg (Ed.), *The Macaques: Studies in Ecology, Behavior and Evolution* (pp. 10–30). New York: Van Nostrand.

Delson, E., & Frost, S. R. (2004). *Paradolichopithecus*: A large-bodied terrestrial papionin (Cercopithecidae) from the Pliocene of western Eurasia (abstract). *American Journal of Physical Anthropology, Supplement 38*, 85.

Delson, E. & Plopsor, D. (1975). *Paradolichopithecus*, a large terrestrial monkey (Cercopithecidae, Primates) from the Plio-Pleistocene of southern Europe and its importance for mammalian biochronology. In *Proceedings VIth Congress of the Regional Committee on Mediterranean Neogene Stratigraphy*, Bratislava, 1975 (pp. 91–96). Slovak Academy of Sciences.

Delson, E., Terranova, C. J., Jungers, W. L., Sargis, E. J., Jablonski, N. G., & Dechow, P. C. (2000). Body mass in Cercopithecidae (Primates, Mammalia): Estimation and scaling in extinct and extant taxa. *Anthropological Papers of the American Museum of Natural History, 83*, 1–159.

Delson, E., Alba, D. M., Frost, S. R., Harcourt-Smith, W. E., Martín Suárez, E., Mazelis, E. J., et al. (2014). *Paradolichopithecus*, a large terrestrial Pliocene cercopithecine from Europe: new remains and an update (abstract). In M. Delfino, G. Carnevale & M. Pavia (Eds.), *Abstract book and field trip guide*, 12th Annual Meeting of the European Association of Vertebrate Palaeontologists, Turin, Italy, June 2014 (p. 50).

Delson, E., Nomade, S., Sen, S., Debard, E., Pastre, J-F., Bahain, J-J. et al. (2024). Geochronology of Senèze: $^{40}Ar/^{39}Ar$ Dating and Magnetostratigraphy, with Notes on an ESR/U-Series Dating Attempt. In E. Delson, M. Faure & C. Guérin (Eds), *Senèze: Life in Central France two million years ago. Paleontology, geochronology, stratigraphy and taphonomy* (pp. 99–122). Cham (Switzerland): Springer.

Depéret, C. (1889). Sur le *Dolichopithecus ruscinensis* nouveau singe fossile du Pliocène du Roussillon. *Comptes Rendus de l'Académie des Sciences* (Paris), *109*, 982–983.

Depéret, C. (1928). Les singes fossiles du Pliocène de France. *Comptes-Rendus du XIV^e^ Congrès Géologique International, 1926* (pp. 3–4). Madrid: Gráficas Reunidas.

Depéret, C. (1929). *Dolichopithecus arvernensis* Depéret: Nouveau singe du Pliocène supérieur de Senèze (Haute-Loire). *Travaux du Laboratoire de Géologie de la Faculté des Sciences de Lyon*, fascicule *15* (mémoire 12), 5–12.

Erxleben, J. C. P. (1777). *Systema regni animalis. Classis 1, Mammalia*. Lipsiae: Weygand.

Fleagle, J. G., & McGraw, W. S. (1999). Skeletal and dental morphology supports diphyletic origin of baboons and mandrills. *Proceedings of the National Academy of Sciences of the USA, 96*, 1157–1161.

Fleagle, J. G., & McGraw, W. S. (2002). Skeletal and dental morphology of African papionins: Unmasking a cryptic clade. *Journal of Human Evolution, 42*, 267–292.

Fooden, J. (2007). Systematic review of the Barbary macaque, *Macaca sylvanus* (Linnaeus, 1758). *Fieldiana Zoology, 113*, 1–60.

Frost, S. R., Ting, N., Harcourt-Smith, W., & Delson, E. (2005). Positional and locomotor behavior of *Paradolichopithecus arvernensis* as inferred from the functional morphology of the postcrania (abstract). *American Journal of Primatology, 66*, 134.

Geoffroy Saint-Hilaire, E. (1812). Tableau des quadrumanes, 1: Ord. Quadrumanes. *Annales du Muséum d'Histoire naturelle, Paris 19*, 85–122.

Gilbert, C. C. (2007). Craniomandibular morphology supporting the diphyletic origin of mangabeys and a new genus of the *Cercocebus*/*Mandrillus* clade, *Procercocebus*. *Journal of Human Evolution, 53*, 69–102.

Gilbert, C. C. (2013). Cladistic analysis of extant and fossil African papionins using craniodental data. *Journal of Human Evolution, 64*, 399–433.

Gray, J. E. (1821). On the natural arrangement of vertebrose animals. *London Medical Repository, 15*, 296–310.

Hoffstetter, R. (1977). Phylogénie des primates. *Bulletin et Mémoires de la Société d'Anthropologie de Paris, 13*, 327–346.

Jolly, C. J. (1967). The evolution of the baboons. In H. Vagtborg (Ed.), *The Baboon in medical research* (Vol. 2) (pp. 23–50). Austin: University of Texas Press.

Kostopoulos, D. S., Guy, F., Kynigopoulou, Z., Koufos, G. D., Valentin, X., & Merceron, G. (2018). A 2Ma old baboon-like monkey from northern Greece and new evidence to support the *Paradolichopithecus - Procynocephalus* synonymy (Primates: Cercopithecidae). *Journal of Human Evolution, 121*, 178–192.

Lacépède, B. G. E. (1799). Tableau des divisions, sous-divisions, ordres et genres des mammifères. In G. L. L. de Buffon (Ed.), *Histoire naturelle* (vol. 38, Quadrupèdes t. 14, pp. 144–195). Paris: P. Didot L'Ainé et Firmin Didot.

Le Maître, A., Guy, F., Merceron, G., & Kostopoulos, D. S. (2023). Morphology of the bony labyrinth supports the affinities of *Paradolichopithecus* with the Papionina. *International Journal of Primatology, 44*, 209–236.

Linnaeus, C. (1758). *Systema naturae per regna tria naturae, secundum classes, ordines, genera, species cum characteribus, differentiis, synonymis, locis* (10th Edn.) Holmiae: Laurentii Salvii.

Maschenko, E. N. (1994). *Papio* (*Paradolichopithecus*) *suschkini* (Trofimov) - revision of systematics, morphofunctional peculiarities of the skull and lower jaw (in Russian). In L. P. Tatarinov (Ed.), *Paleotheriology* (pp. 15–57). Nauka.

Maschenko, E. N. (2005). Cenozoic primates of Eastern Eurasia (Russia and adjacent territories). *Anthropological Science, 113*, 103–115.

Mivart, St. G. (1864). Notes on the crania and dentition of the Lemuridae. *Proceedings of the Zoological Society of London, 1864*, 611–648.

Moyà Solà, S., Pons Moyà, J., & Köhler, M. (1990). Primates catarrinos (Mammalia) del Neógeno de la península Ibérica. *Paleontologia i Evolució, 23*, 41–45.

Necrasov, O., Samson, P., & Rădulesco, C. (1961). Sur un nouveau singe catarrhinien fossile, découvert dans un nid fossilifère d'Olténie (R. P. R.). *Analele Stiintifice Universitatii "Al. I. Cuza" din Iaşi*, Sec. *II, Stiinte Naturale, 7*, 401–416.

Nishimura, T. D., Takai, M., & Maschenko, E. (2007). The maxillary sinus of *Paradolichopithecus sushkini* (late Pliocene, southern Tajikistan) and its phyletic implications. *Journal of Human Evolution, 52*, 637–646.

Nishimura, T. D., Senut, B., Prieur, A., Treil, J., & Takai, M. (2009). Nasal architecture of *Paradolichopithecus arvernensis* (late Pliocene, Senèze, France) and its phyletic implications. *Journal of Human Evolution, 56*, 213–217.

Nishimura, T. D., Zhang, Y., & Takai, M. (2010). Nasal anatomy of *Paradolichopithecus gansuensis* (Early Pleistocene, Longdan, China) with comments on phyletic relationships among the species of this genus. *Folia Primatologica, 81*, 53–62.

Nishimura, T. D., Ito, T., Yano, W., Ebbestad, J. O. R., & Takai, M. (2014). Nasal architecture in *Procynocephalus wimani* (Early Pleistocene, China) and implications for its phyletic relationship with *Paradolichopithecus*. *Anthropological Science*, *122*, 101–113.

O'Shea, N., Delson, E., Pugh, K. D., & Gilbert, C. C. (2016). Phylogenetic analysis of *Paradolichopithecus*: Fossil baboon or macaque? (abstract). *American Journal of Physical Anthropology, S62*, 244.

Owen, R. (1843). Report on the British fossil Mammalia (Part I: Unguiculata and Cetacea). In *Report on the l2th meeting of the British association for the advancement of science for 1842* (pp. 54–74). London: John Murray.

Plastiras, C., Kostopoulos, D. S., & Merceron, G. (2017). Tooth morphology, molar enamel thickness and dental microwear textural analysis with application on European *Paradolichopithecus*/*Procynocephalus* and comparisons with Pleistocene papionins (abstract). In *2nd international meeting of early-stage researchers in paleontology, 2017, Book of Abstracts* (pp. 161–162). http://www.imerp2.upatras.gr/files/mariatest/2IMERP_BOOK_OF_ABSTRACTS.pdf.

Qiu, Z., Deng, T., & Wang, B. (2004). Early Pleistocene mammalian fauna from Longdan, Dongxiang, Gansu, China. *Palaeontologica Sinica, 191. New Series C, 27*, 1–198.

Radinsky, L. (1974). The fossil evidence of anthropoid brain evolution. *American Journal of Physical Anthropology, 41*, 15–27.

Radović, P., Lindal, J., Marković, Z., Alaburić, S., & Roksandic, M. (2019). First record of a fossil monkey (Primates, Cercopithecidae) from the Late Pliocene of Serbia. *Journal of Human Evolution, 137*, 102681.

Radović, P., Marković, Z., Alaburić, S., & Roksandic, M. (2024) A new papionin molar (Primates, Cercopithecidae) from the Pliocene of Serbia. *Paläontologische Zeitschrift*, *98*, 637–646.

Rowe, N., & Meyers, M. (Eds.). (2016). *All the World's primates*. Pogonias Press.

Schaub, S. (1943). Die oberpliocaene Säugetierfauna von Senèze (Haute-Loire) und ihre verbreitungsgeschichtliche Stellung. *Eclogae Geologicae Helvetiae*, *36,* 270–289.

Schlosser, M. (1924). Fossil primates from China. *Palaeontologica Sinica, 1* (2), 1–16.

Sianis, P. D., Athanassiou, A., Kostopoulos, D. S., Roussiakis, S., Kargopoulos, N., & Iliopoulos, G. (2023). The remains of a large cercopithecid from the Lower Pleistocene locality of Karnezeika (southern Greece). *Earth and Environmental Science Transactions of the Royal Society of Edinburgh, 114*, 177–182.

Simionescu, I. (1930). Vertebratele Pliocene dela Măluşteni (Covurlui). *Academia Româna, Publicaţiunile Fondului Vasile Adamachi,, 9*, 83–136.

Simons, E. L. (1970). The deployment and history of Old World monkeys (Cercopithecidae, Primates). In J. R. Napier & P. H. Napier (Eds.), *Old World Monkeys* (pp. 97–137). London: Academic Press.

Sondaar, P. Y., van der Geer, A. A. E., & Dermitzakis, M. D. (2006). The unique postcranial of the Old World monkey *Paradolichopithecus*: More similar to *Australopithecus* than to baboons. *Hellenic Journal of Geosciences, 41*, 19–28.

Stehlin, H. G. (1923). Die oberpliocaene Fauna von Senèze (Haute-Loire). *Eclogae Geologicae Helvetiae, 18*, 268–281.

Šujan, M., Braucher, R., Chyba, A., Vlačiky, M., Aherwar, K., Rózsová, B., et al. (2023). Mud redeposition during river incision as a factor affecting authigenic $^{10}Be/^{9}Be$ dating: Early Pleistocene large mammal fossil-bearing site Nová Vieska, eastern Danube Basin. *Journal of Quaternary Science, 38*, 347–364.

Szalay, F. S., & Delson, E. (1979). *Evolutionary History of the Primates*. New York: Academic Press.

Teilhard de Chardin, P. (1938). The fossils from locality 12 of Choukoutien. *Palaeontologica Sinica*, *new series C, 5*, 1–50.

Terhune, C. E., Curran, C., Croitor, R., Drăguşin, V., Gaudin, T., Petculescu, A., et al. (2020). Early Pleistocene fauna of the Olteţ River Valley of Romania: Stratigraphic and biogeographic implications. *Quaternary International, 553*, 14–33.

Ting, N., Harcourt-Smith, W. E. H., Frost, S. R., & Delson, E. (2004). Description and analysis of postcranial elements of *Paradolichopithecus arvernensis*: A large bodied papionin from the Pliocene of Eurasia (abstract). *American Journal of Physical Anthropology, S38*, 195.

Trofimov, B. A. (1977). Primate *Paradolichopithecus sushkini* sp. nov. from the Upper Pliocene of the Pamirs Piedmont (preliminary communication). *Journal of the Palaeontological Society of India* (for 1975), *20*, 26–32.

Van der Geer, A. A. E., & Sondaar, P. Y. (2002). The postcranial elements of *Paradolichopithecus arvernensis* (Primates, Cercopithecidae, Papionini) from Lesvos, Greece. *Annales Géologiques des Pays Helléniques, 39*, 71–86.

Verheyen, W. N. (1962). Contribution à la craniologie comparée des primates. *Annales du Musée Royale de l'Afrique Centrale, série in 8vo, Sciences Zoologiques*, *105*, 1–247.

Vlačiky, M. (2009). Výskumy kvartérnych paleontologických lokalít na Slovensku v roku 2009. In Z. Németh, D. Plašienka, L. Šimon, M. Kohút, and Ľ. Iglárová (Eds.) *Nové poznatky o stavbe a vývoji Západných Karpát* (Vol. 41, pp. 549–550). Bratislava: Mineralia Slovaca, Geovestník, ŠGÚDŠ. (in Slovak).

Vogel, C. (1966). Morphologische Studien an der Gesichtsschädel Catarrhiner Primaten. *Bibliotheca Primatologica, 4*, 1–226.

Vogel, C. (1968). The phylogenetical evaluation of some characters and some morphological trends in the evolution of the skull in catarrhine primates. In B. Chiarelli (Ed.), *Taxonomy and Phylogeny of Old World Primates with References to the Origin of Man* (pp. 21–55). Turin: Rosenberg and Sellier.